

On Geometric Structure of Point Particles

M. Honda

Plasma Astrophysics Laboratory, Institute for Global Science,
Mie, Japan.

Abstract

I propose, as geometric structure in an internal space, a helical field that is responsible for intrinsic properties of point particles, particularly, electron. For the novel theoretical development, plasma astrophysical analogy is made extensively. Transition between our conventional space and the infinitesimal space is considered in an operational manner. It is shown that rotational eigenvalue equation satisfied by the vector field equivalent to Gromeka-Beltrami flow provides a coordinate-rotor that captures complex orthogonality between the internal coordinate space and isotopic, angular momentum space. Self-consistent normalization of rotational coordinate owing to the rotor is compared to renormalization of electric charge. It is also found that chiral asymmetry of the helical eigenflows can be reflected in electroweak symmetry breaking. The theoretical prototype suggests possible geometrical features of a fundamental framework ruling matters and forces with higher dimensions.

Keywords: Electron · Infinitesimal space · Gromeka-Beltrami flow · Chiral asymmetry · Beta decay · Extra-dimensions

1 Introduction

Reducing elements of matters has been the cutting edge issue on natural philosophy and science, and in arena of modern physics, substantial theoretical and experimental efforts are devoted to unveiling quarks and leptons [1]. Let us focus on the electron that can be isolated stably. As it stands, one has none of observational evidence of the element-divided substructure; upper limit of the radius is reported 10^{-20} cm [2, 3]. According to a great success of quantum electrodynamics (QED) for point particles, we can hardly imagine the electron as a (composite) particle having finite spread, despite its non-zero form factor

for anomaly of magnetic dipole moment. The issue of inner structure could be related to the hierarchy problem [4, 5], which still remains unsolved. The “desert” (e.g., [6]), compatible with the Large Hadron Collider experiments for a decade [7, 8], implies that any responsive feature might not exist down to the spatial scale of around $l_{\text{gut}} \sim 10^{-29}$ cm (corresponding to the grand unification energy; e.g., section 93 in [9]). From the results of ultra-high-energy cosmic ray experiments negative for the “top-down” models (e.g., [10]), there is even a likelihood that the ultramicroscopic featureless landscape continues down to a scale smaller than l_{gut} . In short, the Planck length $l_{\text{P}} \sim 10^{-33}$ cm comes into sight. Unless the electron is made out of any ingredient perceivable in our space-time, we will have, logically, no choice but to conceive that the electric charge $-e$ and spin $1/2$ as the observable attributes reflect structure of another space expanded somewhere in a virtually infinitesimal region. The similar spatio-requirement can also be seen in the string theory that hypothesizes an ingredient having the size of $\sim l_{\text{P}}$; that is, the theory requires extra-dimensions of space (e.g., [11]). From the observational fact that magnetic monopole has not been discovered at all [12, 13], it is simply anticipated that, the mechanism that generates the magnetic moment coupled with the intrinsic angular momentum $\hbar/2$ [14], where $\hbar = h/2\pi$ and h is the Planck constant [15], has an asymmetric relation with the mechanism that generates e , while having a complementary relation with it.

For the challenge of elucidating the structure that engenders those attributes, one of the worthwhile first steps is to find the analogy in structure of nucleon. The nucleon is constantly emitting and absorbing π -meson, to have the boson cloud (e.g., [16]); this picture is similar to the one of electron in QED in which virtual photon dresses it. As for orbital angular momentum \mathbf{L} , the pion cloud entails the eigenvalue of $l = 1$, which means that the pion is *really rotating on an orbit*. Its connection with the spin angular momentum of electron is founded on the local isomorphism between $\text{SO}(3)$ and $\text{SU}(2)$ Lie groups; there is no longer any doubt as to validity of imposing the commutation relation equivalent to that for the operator of $\mathbf{L} = \mathbf{R} \times \mathbf{P}$, on \mathbf{S} [17], where the notations are standard. Accordingly, it will be a decent attempt to envisage, for generation principle of \mathbf{S} , a rotational coordinate of the space expanded in the infinitesimal region of $\|\mathbf{R}\| \rightarrow 0$. However, primitive question of like what coordinate must be rotated has hitherto remained unanswered (e.g., [18]).

It is not totally absurd to look for, further in macroscopic objects, a clue to the puzzle, since the asymmetry of the electromagnetic attributes is being cast to predominance of magnetic fields over cosmological scales (e.g., [19]). It is plasma physics that accounts for the dynamics of many-body system of charged particles coupled with abelian and non-abelian gauge fields [20]. In the context, it is better to seek out, in magnetohydrodynamical features of abelian plasma, an intuitive image for the \mathbf{S} generation. Now, we closer look at the astrophysical jets, which are launched from active galactic nuclei including black holes, to extend splendidly up to million light years. Intriguingly, in the jets one can find some signatures of helical motion as well as helical

structure of magnetic field [21]. Such structure could appear when the plasma attains an energy relaxed state, mostly conserving magnetic helicity [22, 23]. Actually, helical magnetic field structure observed in, for example, interplanetary magnetic clouds [24] and plasma ejecta in the solar corona [25] has been interpreted as exhibiting the relaxed state. Therefore, the structure formation is supposed to be a class of universal magnetohydrodynamic phenomenon. In this aspect, reminding that the pion can be regarded as the lowest energy excitation state of vacuum [26, 27], we genuinely conjecture that the helical structure will reflect the geometrical structure that generates an internal coordinate connecting to \mathbf{S} . Here, it is amusing to compare the galactic nucleus to one neutron, invoking the nuclear reaction of $n^0 \rightarrow p^+ + \pi^-$, where p^+ and π^- are proton and π^- -meson, respectively: making a spinning black hole [28] and accretion disk [29] correspond, respectively, to p^+ and its π^- cloud leads to the apparent correspondence between a bipolar jet and lepton pair emitted in decay of π^- , in parallel with the conjecture. Either way, it seems as if the structure in the infinitesimal space and outer space was described by common geometry — this is original motivation of the present study.

The crucial thing, that divergence difficulty incidental to electron can be successfully removed by the well-defined renormalization of QED, implies latency of a fundamental operation allied with transition to the infinitesimal space. If Nature is essentially inventive, geometry of the space would be to provide the physical meaning of degree of charge renormalization, which has been unknown [30]. Meanwhile, polarization picture of QED vacuum, itself, suggests that one could by no means reach generation principle of e within theoretical framework tacitly involving the vacuum permittivity *ab ovo*. This facet is prominent in the logical base of Lorentz invariant quantum theory of gauge fields [31] such that existence of photon with the speed c results necessarily from charge conservation and local gauge invariance consistent with causality. Put another way, the inherent problem is that the theory is dependent on background. By taking a hint from this impasse *per se*, a naïve attempt is made here to find out a form of the concerned operation: we anticipate a symptom of that form in the macroscopic dielectric distribution by which phase velocity of light spatially changes. The small deviation from c is suggestive of the vacuum polarization effect. It is, by contrast with the magnetohydrodynamical analogy for spin generation, a matter of having an insight into collective phenomena of plasma as dielectric medium [32], among others, dispersion of light propagating through the plasma.

Of course, it is impossible, from plasma physics with U(1) symmetry, to *literally* derive the microscopic mechanics assigning the point the intrinsic quantized attributes. The mechanics is thought of as being rather inaccessible by traditional group theories. For example, the Poincaré group for relativity provides classification of elementary particles [33], but fails in determining their mass as an invariant of the Casimir operator of the group; it all comes down to the problem of free-particle self-energy. In this aspect, worth trying is, away from algebraic approach, an analytic one capable of yielding specific

numerical outputs such as the root of special functions [30]. In the current context, when analytical description of plasmas as the dielectric and magnetofluid is *appropriately generalized and abstracted*, we may get a fortuitous chance to encounter a hopeful candidate for the geometry that engenders e and h . If the framework provides radical representation of space-time independently of background, it would be to encompass generation mechanism of the dimensionless constant including c : $e^2/2hc = e^2/q_p^2 = \alpha$ [34], and its relation to the other interactions. Mechanics in the infinitesimal space should describe observable phenomena of particles and fields in the infinite limit. Thus, priority task is to specify the space-transformation operation responsible for the reproducibility.

In this Perspective Paper, we study, for heuristic, the geometric structure of point(-like, at present stage of knowledge) particles including the electron, and fundamental interactions inseparable from them. Along with the analogy of optical dispersion of plasma, I propose a simple form of the transformation that describes transition to the space expanded in the infinitesimal region. I provide the realistic space, which is spanned by a unific rotational field equivalent to Gromeka-Beltrami vector flow [35] with cylindrical geometry. The infinitesimal realistic space differs from an infinitesimal element of four-dimensional space-time, and also from conventional abstract (internal) space such as isospin space.¹ The field is found to obey the rotational eigenvalue equation, which captures the complex orthogonality between the internal coordinate space and angular momentum space. I address that complementary rotation of coordinates in these isotopic spaces can be reflected in observed spin-precession of electron. We also argue that the electromagnetic coupling is internally determined by a left-handed rotational eigenmode, and this property is linked to parity violation in the β -decay [36, 37]. This eigenmode regulates helical structure of the rotational field. The related geometry is found to be the same as that to describe the helical structure of the relaxed plasma. It is pointed out that the geometrical theory is distinct from the previous morphology in [38], which was constructed within, basically, the conventional framework of plasma physics.

This paper is organized as follows: Section 2 is prepared to give operational tool as a part of the geometric theory. We review the optical dispersion of plasma (Sect. 2.1), in order to arrange a rule of the wavenumber transformation of light accompanying plasma nonuniformity (Sect. 2.2). Taking the abstracted form into account, I propose the spatial transformation to the infinitesimal space of particles (Sect. 2.3). To see its availability, in Sect. 3 we call quark condensate, as it resembles a massive photon state owing to collective oscillatory behavior of plasma electrons. We reproduce the potential detected inside [39] (Sect. 3.1) and outside meson [40] (Sect. 3.2), clarifying a signature of the infinitesimal realistic space spanned by harmonic field. In Sect. 4, I provide an internal module representation of the β -decay products. Making reference to the magnetohydrodynamic details, we geometrically extend the scalar form, and obtain the rotational eigenvalue equation that

¹However, I use the terminology “internal space” (or “internal ...”) throughout, for convenience.

governs vector field spanning that space (Sect. 4.1). The equation is solved as a boundary value problem; we find the eigenfunctions the lepton pairs should internally refer to (Sect. 4.2). The eigenmode property including chiral asymmetry is summarized, and the module representation made of the rotational vector fields is proposed (Sect. 4.3). The eigenmode representing the weak is also provided (Sect. 4.4). In Sect. 5, we treat major issues on observation of the rotational field of charged leptons, in terms of application of the operational formalism to it. In particular, we focus on geometrical mechanics for cyclotron motion of a single electron (Sect. 5.1). From the rotational eigenvalue equation governing the field, we derive a mathematical symbol that sustains the mechanics (Sect. 5.2). Then, we relate the mechanical process renormalizing an internal coordinate to the charge renormalization (Sect. 5.3). For the sake of reinforcing the theory, Sect. 6 is added wherein its compatibility with the standard model is further examined. First, I provide an explanation of how the mechanics could respond to fractional charge of quark [41] (Sect. 6.1). Second, we argue the compatibility with the established model of vacuum [42] (Sect. 6.2), and third, provide a notion of rotational eigenmode coupling responsible for the electroweak coupling [43–45] (Sect. 6.3). Finally, Sect. 7 is devoted to concluding remarks.

2 Abelian Plasma Analogy for an Abstract Form of Spatial Transformation

It is known that classical field theory appropriately provides physical elements to understand the quantum field theory (e.g., [46]) that any modern approach to theories of fundamental interactions rests on. In what follows, propagation of light in spatially nonuniform plasma is considered, as an analogy for the non-trivial transformation involved in the novel theory compatible with the quantum field theory.

2.1 Brief Review of Massive Photon Picture for Plasma Dielectric Response

Begin with considering a discharged gas distributing in vacuum, which comprises freely moving electrons and the charge compensating ions. Light propagating through it induces currents carried mainly by the electrons having the small inertia, whereupon this effect is fed back to the light. The interaction gives rise to optical dispersion. For the phenomenological description, one calls the Maxwell equation in vacuum, taking the free currents into account. For simplicity, provided that the background ions are immovable, the current formation is considered which involves harmonic oscillation of the nonrelativistic electrons that experience a single force $-e\mathbf{E}$, where \mathbf{E} is the self-consistent electric field. In this model, one has the Klein-Gordon equation for transverse

electromagnetic field of $\Phi = \{\mathbf{E}, \mathbf{B}\}$ [47]:

$$(\partial^2/\partial t^2 - c^2\Delta)\Phi = -(ne^2/m_e)\Phi, \quad (1)$$

where $\Delta = \nabla^2$, and n and m_e are the plasma density and the electron rest mass, respectively. When assuming the plasma and plane wave to be infinitely pervading the vacuum, equation (1) immediately gives the dispersion relation of the electromagnetic wave having its angular frequency ω and wavenumber \mathbf{k} :

$$\omega^2 = c^2\mathbf{k}^2 + \omega_p^2, \quad (2)$$

where ω_p is the plasma frequency that satisfies $\omega_p^2 = ne^2/m_e$ [48]. For (2), the refractive index is given by $ck/\omega = \sqrt{1 - (\omega_p^2/\omega^2)}$, where $k = \|\mathbf{k}\|$. On both sides of (2), we multiply \hbar^2 , and put $E = \hbar\omega$ and $\mathbf{p} = \hbar\mathbf{k}$. Then, the relativistic relation comes out, to give $E^2 = c^2\mathbf{p}^2 + m^2c^4$ [49], where m is defined by $m = \hbar\omega_p/c^2$, which has dimension of mass. This suggests that the photons behave as though they had the mass, as in superconductors [26, 32].

The real position vector \mathbf{R} of the harmonic oscillator, which assigns the photons m , is parallel to \mathbf{E} (perpendicular to magnetic field \mathbf{B}), on account of $\mathbf{R} = (e/k_s)\mathbf{E}$, where $k_s = m_e\omega^2$ can be identified with the spring constant. This means that, when regarding k_s/e as a constant Λ , equation (1) with the following replacement results in describing the coordinate wave that traces position of the electrons:

$$\mathbf{E} \longrightarrow \Lambda\mathbf{R}, \quad \mathbf{B} \longrightarrow i\Lambda\mathbf{R}, \quad (3)$$

where $i = \sqrt{-1}$. Equation (3) seems to expose a hidden transformation form generating internal rotational coordinate of electron, in accord with the electron picture mentioned above. Besides, a view of the coordinate wave is reminiscent of general coordinate transformation of space-time [50] (see [51], for the terminology).

2.2 Wavenumber Transformation of Light

2.2.1 Elementary Excitation Representation of a Propagative Massive Photon

The nonuniformity of plasma, which varies phase velocity of the light, is taken into consideration. For instance, as shown in Fig. 1(a), we set two distinct regions: high density region I specified by the plasma frequency of ω_{p1} and low density region II by that of $\omega_p (< \omega_{p1})$, in the way that on an infinite boundary surface, these come in contact with one another. Monochromatic light with $\omega (> \omega_{p1})$ propagating through the region I in the direction normal to the contact surface is transmitted to the region II across the surface. Provided that ω is unchanged in the entire process, the dispersion relations in the region I and II can be written as $\omega^2 = c^2k^2 + \omega_{p1}^2$ and $\omega^2 = c^2k_2^2 + \omega_p^2$, respectively.

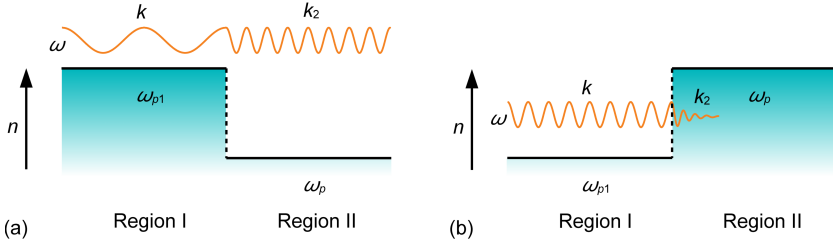


Fig. 1 Schematics of the wavenumber transformation $k \rightarrow k_2$, which comes about when light (wavy solid curves) propagates from plasma region I to II across the boundary (dashed lines): a surface of discontinuity of the density n (solid lines). Provided the angular frequency of the light ω is invariant for the transformation, the cases of $\omega_p < \omega_{p1} < \omega$ (a) and $\omega_{p1} < \omega < \omega_p$ (b) are shown, where ω_{p1} and ω_p denote the plasma frequency of the region I and II, respectively.

By combining them, we obtain, for positive real wavenumber transformation of $k \rightarrow k_2$, the factorized representation of k_2 :

$$k_2 = \sqrt{\left(k^2 + \frac{\omega_{p1}^2}{c^2}\right) \left(1 - \frac{\omega_p^2}{\omega^2}\right)}. \quad (4)$$

Note that the second factor of the right-hand side (RHS) indicates the refractive index: $\tilde{n} = ck_2/\omega$ in the region II.

Here, suppose the situation in which keeping the ratio of ω_p/ω constant, $\omega \downarrow \omega_{p1}$ is taken to give $k \rightarrow 0$. For given definitions of $\mu = k_2(k=0)$, $\bar{\mu} = \omega_{p1}/c$, and $\delta = \omega_p^2/\omega_{p1}^2$, the wavenumber transformation can be expressed as

$$k(=0) \longrightarrow \mu = \bar{\mu}\sqrt{1-\delta}. \quad (5)$$

Equation (5) can be regarded as representing creation of a propagative photon having the mass of $m = \hbar\bar{\mu}/c$. Particularly, in the case for which $\delta \ll 1$, the phase velocity in the region II, c/\tilde{n} , is approximately given by $c(1 + \delta/2)$, so that it slightly deviates from c . The form is that as we have desired; equation (5) is expected to be related with the lowest energy excitation of real particles.

It is noticed that, when comparing the massive photon to a real matter particle, we should take the group velocity of the light into consideration. The lowest energy excitation with $c^{-1}\|\partial\omega/\partial k\| = \beta (< 1) \rightarrow 0$ can be translated into unambiguous separation of the kinetic energy $[(\Gamma - 1)mc^2]_{\Gamma \rightarrow 1}$ from the total energy $E = [\Gamma mc^2]_{\Gamma \rightarrow 1}$, where $\Gamma = (1 - \beta^2)^{-1/2}$. This can be compared to transition from $\sqrt{E^2(\|\mathbf{p}\|=0)/c^2} = mc$ to the nonrelativistic momentum $[\beta mc]_{\beta \rightarrow 0}$. The formalism suggests that $\bar{\mu} = \sqrt{\omega^2(k=0)/c^2} = mc/\hbar$ should be replaced by $[\beta mc/\hbar]_{\beta \rightarrow 0}$ with the value remaining finite.

2.2.2 Elementary Excitation Representation of a Non-propagative Massive Photon

The density profile is inverted with respect to the propagation direction of the light. As shown in Fig. 1(b), we configure low density region I with the plasma frequency of ω_{p1} and high density region II with $\omega_p (> \omega_{p1})$ such that an infinite contact surface separates them. The light with $\omega (> \omega_{p1})$ propagating through the region I normally incidents on the surface, to be transmitted to the region II. Here, we consider the situation in which the transmitted light decays because of $\omega < \omega_p$. For the dispersion relations same as given above, we obtain, for $k \rightarrow k_2$, the following representation of k_2 :

$$k_2 = -i(\omega_p/c) \sqrt{1 - (\omega^2/\omega_p^2)}, \quad (6)$$

making the negative sign have the physical meaning that a damping solution has been chosen. Again keeping the ratio of ω/ω_p , $\omega \downarrow \omega_{p1}$ is taken to give $k \rightarrow 0$, and then, the wavenumber transformation can be expressed as

$$k (= 0) \longrightarrow \mu = -i\bar{\mu}^* \sqrt{1 - \delta} =: -i\mu^*, \quad (7)$$

where $\bar{\mu}^* = \omega_p/c$, $\delta = \omega_{p1}^2/\omega_p^2$, and $m^* = \hbar\bar{\mu}^*/c$, which stands for mass of non-propagative photon. Equation (7) is expected to be related with the lowest energy excitation of virtual particles.

2.3 Transformation Between Our Conventional Space and Infinitesimal Space

The wavenumber transformation of the massive photon is coupled with coordinate of the propagation direction, to generate phase transformation of Φ between the region I and II. This feature provides a useful analogy for the transformation between the concerned internal space and the \mathbf{R}^3 real-space from which observer looks into the internal one. The spatial transformation should be related to the generation of wavefunction of particle, which coincides with potential development in the \mathbf{R}^3 . As seen later, it does *not* mean that the transformation (compared to the scalar form) by itself constitutes geometrical main body. Anyway, let us consider a generic form of three-dimensional isotropic potential $V(\xi')$, and suppose that it is centered at coordinate origin $O : (X, Y, Z) = (0, 0, 0)$ in the flat (locally Euclidean) \mathbf{R}^3 , where the dimensionless, positive real argument is defined as $\xi' = \bar{\mu}\|\mathbf{R}\| = \bar{\mu}R \notin \{0, +\infty\}$. For an equipotential surface of $R = \sqrt{X^2 + Y^2 + Z^2} = \xi'/\bar{\mu}$, a circle having the dimensional radius R can be put on the equatorial plane $Z = 0$. This locus is described by the simple blowup:

$$\tilde{X} = \bar{\mu}R \cos \theta' = \xi' \cos \theta', \quad \tilde{Y} = \bar{\mu}R \sin \theta' = \xi' \sin \theta', \quad (8)$$

and dimensionless equation of the circle is given by

$$\tilde{X}^2 + \tilde{Y}^2 = \xi'^2. \quad (9)$$

Domain of definition for $V(R)$ is given by $R > \epsilon$: in the domain, $\bar{\mu}R$ indicates a well-defined real value of ξ' . On the other hand, in the region of $R \leq \epsilon$ off the domain, we suppose that indetermination led by $R \rightarrow 0$ sets in, and require discontinuous transition from (9) to

$$\tilde{X}^2 + \tilde{Y}^2 = 0, \quad (10)$$

for $\|\tilde{X}\| \rightarrow 0$ and $\|\tilde{Y}\| \rightarrow 0$, as would be a decent representation of null-radius associated with point particles. It is trivial that the singular region (10) does not belong to the Euclidean \mathbf{R}^3 -space anymore; the Pythagorean theorem is violated. Definition of neighbourhood in standard analysis leads to $\{\mathbf{R} \mid R < \epsilon\} = \emptyset$, which means that the Euclidean space is locally punctured. For the topological modeling, there is a physical reasoning that could convince us of its feasibility.

We reconsider the non-propagative photon characterized by the real mass $m^*(\neq 0)$, real energy $E (< m^*c^2)$, and imaginary momentum \mathbf{p}_i . For the relativistic dispersion, instead of normal transformation from the elliptic to hyperbolic (timelike) form, here we should make the one to null-vector form, that is, the transition from the virtual particle state having a real $p^* = \|\mathbf{p}_i\|$ into massless state:

$$(E/c)^2 + p^{*2} = (m^*c)^2 \longrightarrow (E/c)^2 + p^{*2} = 0. \quad (11)$$

For, this can naturally be made to correspond to (9) \rightarrow (10), albeit apparently breaking the Lorentz symmetry. The transition of (11) with $E/c \rightarrow 0$ and $p^* \rightarrow 0$ actually allows for replacement of $E/c \rightarrow \mathbf{p}$ and $p^* \rightarrow i\mathbf{p}$, with \mathbf{p} being a real three-dimensional vector. The massless particle having the momentum \mathbf{p} whose magnitude indicates E/c is definitely an entity observed as photon in vacuum. Hence, the (11) accommodated by the replacement is a physically possible process as spatial transfer from the dispersive medium to the vacuum.

The singular region in the \mathbf{R}^3 , characterized by (10), is defined as indeterminate region. In correspondence to what observer can never jump on internal coordinate of the massless photon, namely, the causal disconnection, the \mathbf{R}^3 spanned by $V(R)$ can not exist in the indeterminate region due to the definition. Nevertheless, on the analogy of the replacement by which to access to the eigenstate of the photon, we can figure out the spatial transformation to access to internal coordinate intrinsic to particles. That is, for (9) \rightarrow (10), the following replacement invoking a basis vector $\hat{\mathbf{x}}$ could hold:

$$\tilde{X} \sim \cos \theta' \longrightarrow \hat{\mathbf{x}}, \quad \tilde{Y} \sim \sin \theta' \longrightarrow i\hat{\mathbf{x}}. \quad (12)$$

When introducing the orthogonal basis vector $\hat{\mathbf{y}}$ that satisfies $\hat{\mathbf{y}} = i\hat{\mathbf{x}}$, we obtain $\tilde{Y} \rightarrow \hat{\mathbf{y}}$. As is, it turns out that equation (12) prompts leap from the real XY -plane to Wessel-Argand-Gauß (complex) plane, settling $\hat{\mathbf{x}}$ and $\hat{\mathbf{y}}$ as the axes. This plane exists in $\mathbf{r}^3 \times \mathbf{r}^3$ host space as the *point* (as an element) of complex three-dimensional space: $\hat{\mathbf{x}} + i\hat{\mathbf{y}} = \mathbf{0}$, sustaining orthogonality of the two \mathbf{r}^3 -real spaces. Note here that the \mathbf{r}^3 should be distinguished from \mathbf{R}^3 , as is unable to define the norm $\|\mathbf{R}\|$. The internal \mathbf{r}^3 - or $\mathbf{r}^3 \times \mathbf{r}^3$ -space is referred to as infinitesimal realistic space (or infinitesimal space); the peculiar complex space $\{\mathbf{0}\}$ is supposed to be in the indeterminate region. In terms of the specific setting, therefore, the infinitesimal space is distinguished from conventional compactified space, though their geometrical connection may be anticipated (cf. Sect. 5.3).

On the complex plane, we have $\zeta = \tilde{x} + i\tilde{y}$ with \tilde{x} and \tilde{y} being real, and give $(\tilde{x}, \tilde{y}) = (\xi \cos \theta, \xi \sin \theta)$ as with (8). For $(\tilde{X}, \tilde{Y}) \rightarrow (\tilde{x}, \tilde{y})$, we suppose the linear transformation of $(\theta', \xi') \rightarrow (\theta, \xi)$ of the form: $\theta'/g_0 \rightarrow \theta$ and $\xi'/g_0 \rightarrow \xi$ with $g_0 = 2$, in consideration of the multiplicity of \mathbf{r}^3 and loop continuity of $2\pi\xi' = g_0(2\pi\xi)$. Putting $\xi = kr$ provided $\zeta \in \mathbb{C}_* \subseteq \{\tilde{z} \in \mathbb{C} \mid \tilde{z} \neq 0, \infty\}$, $\xi' \rightarrow g_0\xi$ is cast to the expression of $\bar{\mu}R(=\infty \cdot 0) \rightarrow g_0kr$, where the left-hand side (LHS) including the round bracket represents that for $R \rightarrow 0$ and $\bar{\mu} \rightarrow \infty$, $\bar{\mu}R$ is in the indeterminate region, manifesting extension of the number system of $\mathbb{R}_* := \{-\xi', \xi'\} \subset \mathbb{R}$. Noted is that \mathbb{C}_* stands for an open subset of the finite complex numbers, and \mathbb{R}_* the open set of the finite real numbers. Formally introducing $g = g_0\sqrt{1 - \delta}$ with δ being a parameter, we have

$$\mu R(=\infty \cdot 0) \rightarrow gkr, \quad (13)$$

where $\mu = \bar{\mu}\sqrt{1 - \delta}$. Equations (12) and (13) can be understood as a feasible form of transformation from the \mathbf{R}^3 space to the infinitesimal $\mathbf{r}^3 \times \mathbf{r}^3$ space, along the extension: $\mathbb{R}_* \cup \{\pm\infty\} \left(\supset \left\{ \frac{\pm\xi'}{\pm\infty} \right\} \right) \rightarrow \mathbb{C}_*$ or $\mathbb{R}_* \cup \{\pm 0\} \rightarrow \mathbb{C}_*$, to be involved in transformation from potential function $V(\xi')$ to an internal function dependent on ξ . Here, it is supposed that the extended sets belong to the Affinely extended real number $\bar{\mathbb{R}} = [-\infty, +\infty]$, paralleling the extension of \mathbb{C}_* given below.

We now consider the inverse transformation: $\mathbf{r}^3 \times \mathbf{r}^3 \rightarrow \mathbf{R}^3$ that generates $V(\xi')$ as an output function. For the inverse of (12), we read off the following replacement, invoking a basis vector $\hat{\mathbf{X}}$:

$$\tilde{x} \sim \cos \theta \rightarrow \hat{\mathbf{X}}, \quad i\tilde{y} \sim i \sin \theta \rightarrow -\hat{\mathbf{X}}. \quad (14)$$

As the inverse of (13) in which (14) is involved, a possible form is

$$kr(=0 \cdot \infty) \rightarrow g^{-1}\mu R. \quad (15)$$

Here, the LHS including the round bracket represents that for $k \rightarrow 0$ and $r \rightarrow \infty$, kr is in indeterminate region, manifesting the extension of \mathbb{C}_* (in

the conventional sense). Equations (14) and (15) suggest that in the infinite distance of \mathbf{r}^3 there exists \mathbf{R}^3 , along $\mathbb{C}_* \cup \{0\}$ ($\supset \{\frac{\xi}{0}\}$) $\rightarrow \mathbb{R}_*$ or $\mathbb{C}_* \cup \{\infty\} \rightarrow \mathbb{R}_*$. The limit of $k \rightarrow 0$, cooperating with $r \rightarrow \infty$, can be interpreted as a projection linked to the foregoing setting of $Z = 0$ in \mathbf{R}^3 .

Equation (15) appears to be of the form that enables us to make $k (= 0)$ and $\mu(\bar{\mu}, \delta)$ correspond to those in (5), and $r = \infty$ to a bulk condition for the plane wave to have the diverging wavelength. As is, we also prepare $\mu(\bar{\mu}^*, \delta)$ with the factorized form same as (7), though $\bar{\mu}$, $\bar{\mu}^*$, and δ herein are, at this moment, regarded as the abstracted symbols. Here, we pay attention to what in (5) $k = 0$ was needed for fixing $\bar{\mu}$, whereas in (7) $\bar{\mu}^*$ was free of k . Besides, since the previous δ could be handled as parameter intrinsic to the elementary excitation in the double plasma, namely plasmon, the corresponding symbolic δ as well is supposed to be a parameter intrinsic to elementary excitation in double (causally disconnected) vacuum. Taking all this into consideration will now convince us of physical relevance of the following proposition: the $\mathbf{r}^3 \times \mathbf{r}^3 \rightarrow \mathbf{R}^3$ transformation related to the lowest energy excitation of real and virtual particle, respectively represented in the form of

$$kr(= 0^{(\prime)} \cdot \infty) \longrightarrow g_0^{-1} \bar{\mu} R^*, \quad (16a)$$

$$kr(= 0 \cdot \infty^{(\prime)}) \longrightarrow g_0^{-1} (-i\bar{\mu}^*) R^* = g_0^{-1} \bar{\mu}^* R, \quad (16b)$$

where the primes in (16a) and (16b) signify that $k \rightarrow 0$ and $r \rightarrow \infty$ take the lead in the indetermination, along $\mathbb{C}_* \cup \{0\}$ and $\mathbb{C}_* \cup \{\infty\}$, respectively. The quantities $\bar{\mu}$ and $\bar{\mu}^*$ are related to observable mass m of real and virtual particle, by $\bar{\mu} = [\beta mc/\hbar]_{\beta \rightarrow 0}$ and $\bar{\mu}^* = mc/\hbar$, respectively, where $\beta = c^{-1}(\partial E/\partial p)$.

In general, distinguishing indeterminate forms (and comprehensive treatment of number systems) could be a subject of nonstandard analysis that invokes hyperreal number. Concerning this, an intuitive explanation for the LHS of (16) is provided by employing, e.g., the Bessel function $J_1(\xi)$:² Adding the points $\{0\}$ and $\{\infty\}$ that never accommodate $J_1(\xi = 0) = 0 = J_1(\xi = \infty)$ because of $\xi \notin \{0, \infty\}$, we allow for $J_1(k \rightarrow 0) \sim \xi/2$ and $J_1(r \rightarrow \infty) \sim \sqrt{2/\pi\xi} \cos(\xi - 3\pi/4)$, which correspond to the regimes of (16a) and (16b), respectively. In this sense, the indetermination is apparent in the internal space, and standard analysis is still legitimate. Relating to this, the foregoing indeterminate form for $\bar{\mu}R$ may be written as $\bar{\mu}R(= \infty \cdot 0^{(\prime)})$, in conformity with (16). This realm would postulate the smaller mass of $\bar{\mu} \ll l_P^{-1}$, viz., $R_S \ll \sim l_P$, where R_S is the Schwarzschild radius [53]. Another realm of $\bar{\mu}R(= \infty^{(\prime)} \cdot 0)$, which implies larger mass, is not discussed here.

²Notation of special functions is as with that in [52] throughout.

3 Feasibility of the Transformation and a Signature of the Infinitesimal Space

3.1 Complex Analytical Consideration on Quark-Antiquark Potential

Prior to application of the spatial transformation to a single fermion, we try exploiting it for a quark pair as a Bose-Einstein condensate closer with the plasmon mentioned above. This orientation is taken to clarify technical feasibility of the transformation operation and, at the same time, a signature of the infinitesimal realistic space. While the composite particle has a finite size as large as classical electron radius, it just embodies a closed \mathbf{R}^3 real-space perfectly shielded from external (our macroscopic) \mathbf{R}^3 -space. The feature confirmed experimentally is found to be well captured by the transformation (16). For convenience, we begin with recalling the β^- -decay reaction: $\nu_e + d \rightarrow e^- + u$, where the notations are standard. For including β^+ -decay, denoting by q (\bar{q}) quark (antiquark) and by ℓ ($\bar{\ell}$) lepton (antilepton), we here give the generic expression of

$$q_L + (\bar{q})_R \rightarrow \ell_L + (\bar{\ell})_R, \quad (17)$$

where the subscripts L and R stand for the left- and right-handed state, respectively.

We aim at associating $k \rightarrow 0$ followed by (16), with the lowest energy excitation of quarks. For the moment, this is intended for a $q\bar{q}$ pair whose motion is nonrelativistic so that $\beta \rightarrow 0$, though the approximation is known to be practically better for heavier mesons, typically quarkonia. We call a basic form of the $q\bar{q}$ potential that has been confirmed for such mesons, namely, the Cornell potential [39]

$$V(R^*) = C_1 R^* - C_{-1} R^{*-1}, \quad (18)$$

where C_1 and C_{-1} are real constants, and $R^* = \|\mathbf{R}^*\|$ is distance between q and \bar{q} in the closed space confining colors. An attention is paid to the fact that this function satisfies the ordinary differential equation of

$$(d^2/dR^{*2} + R^{*-1}d/dR^* - R^{*-2})V = 0. \quad (19)$$

Let us see the bracket of (19) as an operator acting on V . Then, it seems as if exposing a part of the Laplacian for cylindrical coordinate system. In fact, the function of (18) with R replacing R^* amounts to radial part of solution of the Laplace equation in \mathbf{R}^2 cylindrical system (R, Θ) uniform in axial Z -direction, suggesting a specific choice of axes in the \mathbf{R}^2 space such as $\cos \Theta = 1$. On the other hand, we will see no convincing reason for regarding R as radial coordinate of the fictitious cylinder furnished in our \mathbf{R}^3 space. At this juncture, we virtually introduce \mathbf{r}^3 real space to configure the cylindrical system.

Thereupon, we presume the harmonic function $\phi(\mathbf{r})$ in the space, which satisfies $\Delta\phi(r, \theta, z) = 0$. Concerning the solution of the form of $\phi = \eta(r)e^{i(m\theta - kz)}$, we contemplate the equation for η :

$$(d^2/dr^2 + r^{-1}d/dr - m^2/r^2 - k^2)\eta = 0. \quad (20)$$

For the bracket set to $m = \pm 1$, taking $k \rightarrow 0$ compared to $\beta \rightarrow 0$, and simultaneously carrying out replacement of $r \rightarrow R^*$, bring about the operator of (19). Evidently, this procedure entails the function transformation of $\eta(r) \rightarrow V(R^*)$.

This is not mathematical artifact. Real part of the complex function of $\phi(k \rightarrow 0)$, i.e., $\eta \cos \theta$ for $m = \pm 1$, can be virtually compared to electrostatic potential in the \mathbf{R}^2 cylindrical free-space, especially, that proportional to $R \cos \Theta$; $\|\phi\| = \eta$ corresponds to the potential amplitude. On the complex plane spanned by the scalar field $\phi(k \rightarrow 0)$, one can choose a projective axis along which to put the basis vector $\hat{\mathbf{X}}$, such that $\cos \theta \rightarrow \hat{\mathbf{X}}$. Then, $\eta \hat{\mathbf{X}}$ analogous to displacement of circular membrane oscillation (cf. Sect. 4.1) could be regarded as a coordinate vector (like a generalized coordinate in Lagrangian, associated with scalar fields; e.g., [46]). Meanwhile, color electric potential binding $q\bar{q}$ is approximately given by $V(R^*) \propto R^*$ for large R^* [54]. It is thus found that transformation of the potential amplitude, $\|\phi\| \rightarrow V$, can be related to generation of the rotational coordinate along $\eta \hat{\mathbf{X}} \rightarrow \mathbf{R}^*/2$. As for quarks of pion, quadratic (harmonic oscillatory) feature of a rotational parameter of chiral transformation appears in isospin-space [55]. In the context, we envisage that the potential established in the \mathbf{R}^3 space reflects η^2 norm; the relevance is seen later. It should be, here, noted that $k \neq 0$ is necessary for ensuring $\mathbf{r}^3 \neq \mathbf{R}^3$, whereas $k \rightarrow 0$ with $\hat{\mathbf{z}} := \mathbf{k}/k \rightarrow \mathbf{0}/0$ can be compared to the uniformity in an indeterminate Z -direction.

In the (20) divided by k^2 , we put $\xi = kr \notin \{0, \infty\}$. In the general case for which m is integer, two linearly independent solutions to this equation are the modified Bessel functions of order m , $I_m(\xi)$ and $K_m(\xi)$ [in the case of $m \neq$ integer, $I_m(\xi)$ and $I_{-m}(\xi)$]. Hence, $I_{\pm 1}(\xi)$ and $K_{\pm 1}(\xi)$ are in on the current issue. Their asymptotic forms (leading contributions) for the small ξ , in which $k \rightarrow 0$ takes the lead, should be considered each; this secures validity of the linear combination form over the concerned entire ξ -range. It then follows that $k \rightarrow 0$ signifies the projection onto cylindrical base. The scalar function $\phi(k \rightarrow 0)$ as the linear combination of the asymptotic forms constitutes a complex function, which is denoted by $f(\zeta) =: w$. Here, $\zeta = \xi e^{i\theta}$ and $(\xi \cos \theta, \xi \sin \theta) = (\tilde{x}, \tilde{y})$, along the notation in Sect. 2.3.

Letting $u(\xi, \theta)$ and $v(\xi, \theta)$ be real functions, we assume the complex function of $w = u + iv$ to be analytic. Then, u and v satisfy the Cauchy-Riemann equation,

$$\partial u / \partial \xi = \xi^{-1} \partial v / \partial \theta, \quad \xi^{-1} \partial u / \partial \theta = -\partial v / \partial \xi, \quad (21)$$

to be the harmonic conjugates on the $\tilde{x}\tilde{y}$ -plane. Among the linear combinations, a feasible form is found to be $c_1 \lim_{k \rightarrow 0} [I_1(\xi)e^{i(\theta - kz)}] -$

$c_{-1} \lim_{k \rightarrow 0} [K_{-1}(\xi) e^{i(-\theta - kz)}]$, where c_1 and c_{-1} are real constants. That is, we have

$$u = \left(\frac{c_1}{2} \xi - c_{-1} \frac{1}{\xi} \right) \cos \theta, \quad v = \left(\frac{c_1}{2} \xi + c_{-1} \frac{1}{\xi} \right) \sin \theta, \quad (22)$$

which suffice for (21). This indicates that the two modes of $m = \pm 1$ contribute to w ; these call for $\mathbf{r}^3 \times \mathbf{r}^3$ spaces, to be intertwined via the complex plane. In the regime led by $k \rightarrow 0$, the variable ξ can be expressed as $kr (= 0^{(l)} \cdot \infty)$, along (16a). Of importance is to clarify the domain of ξ for (22), that is, the upper limit of ξ by which $r \rightarrow \infty$ is well constrained. The $f(\zeta)$ provides the following form of linear map from the complex plane ζ to w :

$$w = (c_1/2) \zeta - c_{-1} \zeta^{-1}. \quad (23)$$

Note here that the coordinate transformation $f: (\tilde{x}, \tilde{y}) \rightarrow (u, v)$ exhibits singularity at $\tilde{k} = ka = \sqrt{2c_{-1}/c_1}$. For the transformation to be bijective conformal map, $\xi < \tilde{k}$ must be satisfied, so that \tilde{k} can be regarded as the upper limit of ξ . In particular, circular rotation on $\xi = \tilde{k}$ is, in the case of $c_1 c_{-1} > 0$, transformed to oscillation on line segment of imaginary axis connecting $(u, v) = (0, -\sqrt{2c_1 c_{-1}} i)$ to $(0, \sqrt{2c_1 c_{-1}} i)$ on the w -plane. On the other hand, in the case of $c_1 c_{-1} < 0$ (including the Kutta-Joukowski transform [56]), circular rotation on $\xi = \sqrt{-2c_{-1}/c_1}$ is transformed to oscillation on line segment of real axis connecting $(-\sqrt{-2c_1 c_{-1}}, 0)$ to $(\sqrt{-2c_1 c_{-1}}, 0)$. As is, two-valuedness arises on the real axis of the w -plane. It turns out that such a finite domain prohibited for real u does not appear in the former case; therein we give specific definition of \mathbb{C}_* as $\{\zeta \mid 0 < \xi < \tilde{k}\}$.

In the case for which $c_1 c_{-1} > 0$, the real function of $u = \Re(w)$ could appear as the potential (18). It is natural to identify the concerned \mathbf{r}^3 -space with the one that has been provided in Sect. 2.3. For generation of $V(R)$, the lead by $k \rightarrow 0$, along $\mathbb{C}_* \cup \{0\}$, should be involved in the transformation of $\mathbf{r}^3 \times \mathbf{r}^3 \rightarrow \mathbf{R}^3$. Recalling (14), u in (22) is rewritten as $\eta(\xi) \tilde{\mathbf{X}}$, where η stands for real amplitude of the intertwined modes. Now, the transformation of which the type is the same as (16a)

$$\xi := kr (= 0^{(l)} \cdot \infty) \longrightarrow g_0^{-1} \bar{\mu} R^* \quad (24)$$

is applied to $\eta(\xi)$. The generated function for R^* is then found to show the form of (18) the nonrelativistic quantum chromodynamics (QCD) is accountable to (e.g., [57]).

3.2 The Yukawa Potential

If two-valuedness is prohibited on the w -plane, ξ cannot exceed \tilde{k} , as long as $k \rightarrow 0$ takes the lead. This seems to capture characteristic of quark confinement; the ζ -dependence of w to be reflected in the energy-scale dependence of the Wilson's law [58], that is, the first (second) term of the RHS of (23), in the area (perimeter) law. In order to move to region of larger ξ , we should prepare

$\phi(r \rightarrow \infty)$ owing to the lead of $r \rightarrow \infty$: the linear combination of the asymptotic forms of $c_1 \lim_{r \rightarrow \infty} [I_1(\xi)e^{i(\theta-kz)}] - c_{-1} \lim_{r \rightarrow \infty} [K_{-1}(\xi)e^{i(-\theta-kz)}]$. That is, we have

$$\frac{c_1 e^\xi - \pi c_{-1} e^{-\xi}}{\sqrt{2\pi\xi}} \cos \theta + i \frac{c_1 e^\xi + \pi c_{-1} e^{-\xi}}{\sqrt{2\pi\xi}} \sin \theta, \quad (25)$$

with ξ being $kr (= 0 \cdot \infty^{(')})$, along (16b). The indeterminate form manifests that $k \rightarrow 0$ is taken to the extent that the large ξ is well maintained. In this regime, it is found, especially for $c_1/c_{-1} = \pi$, that equation (25) can be cast to the next linear combination form of

$$\left\{ \begin{array}{c} c_1 \\ \pi c_{-1} \end{array} \right\} [I_{1/2}(\xi) \cos \theta + i I_{-1/2}(\xi) \sin \theta]. \quad (26)$$

This indicates that the system spanned by $\phi(r \rightarrow \infty)$ is accommodated by $\theta \rightarrow \theta'/g_0$. As is, we again apply (14) to (26), for $\mathbb{C}_* \cup \{\infty\}$, where $\mathbb{C}_* = \{\zeta \mid \bar{k} < \xi < \infty\}$. The resulting quantity is written as $\eta(\xi)\bar{\mathbf{X}}$ as before, and then, the function η is given by

$$\eta(\xi) = -2 \left\{ \begin{array}{c} c_1/\pi \\ c_{-1} \end{array} \right\} K_{\pm 1/2}(\xi) =: \frac{c_0}{\sqrt{\pi}} K_{\pm 1/2}(\xi). \quad (27)$$

Along the discussion in the previous section, η^{g_0} with $g_0 = 2$ is translated as internal Hamiltonian density of the harmonic oscillation. To the norm, we apply the transformation as with (16b). This results in yielding the energy transformation of

$$\eta^{g_0}(\xi) \longrightarrow \alpha_s \frac{e^{-\bar{\mu}^* R}}{\bar{\mu}^* R} =: \frac{V(R)}{m_\pi c^2}, \quad (28)$$

with $c_0^{g_0} \rightarrow \alpha_s$. Here, α_s is related to the dimensionless constant of g_s^2/q_p^2 , where g_s denotes the coupling strength between pion and nucleon, and $\bar{\mu}^* = m_\pi c/\hbar$ with m_π being the observed pion mass.

According to asymptotic property of $K_{\pm 1}(kr) \sim K_{\pm 1/2}(kr)$ for $r \rightarrow \infty$, the product $\sim c_0^2 K_{-1/2} K_{1/2}$ can be understood as far-field interference between K_{-1} and its counterpart K_1 . In this connection, it is remarked that the same mathematical representation appears in an attractive interaction of plasma elements; formation and interference of dipole magnetic fields characterized by $K_{\pm 1}$ can be seen in self-organization of vortices as two-dimensional structure of plasma turbulence [59] and merging of the vortices [60]. Intermittent activity of galactic nuclei is expected to establish this kind of turbulent state [61, 62], likely followed by transition to an energy relaxed state.

The function of $V(R)$ exposes the potential energy for strong nuclear force [40] being proportional to the scalar field of pion with spin 0. That inertia of the constituent quarks is so small as to degrade nonrelativistic approximation for the motion seems to be reflecting the constraint on $k \rightarrow 0$, contrast to the previous constraint on $r \rightarrow \infty$. Relating to this, $\xi \gtrsim \mathcal{O}(1)$ can be reflected in the region of $R \gtrsim \bar{\mu}^{*-1}$ in which the Yukawa potential appears.

The results obtained in this section support physical validity of introducing, in the infinitesimal space, the cylindrical system with the axis along which to take $k \rightarrow 0$, and the related harmonic functions. The number of $\|m\| = 1$ herein can be identified with magnitude of spin of gluons. What $k = 0$ is prohibited in the system of (20) suggests that quarks could never be at rest.

4 Rotational Field in the Cylindrical System

4.1 Scalar Form on the Base, and the Geometric Extension

From the internal potential representation, we should derive internal representation of (A) onset of the scattering in (17) and (B) the created lepton pairs. To achieve the objective, it will be better to take a strategy different from drawing a representation of *baryonic* fermion from the one of pion [63] (and also, [64, 65]), although the internal pion field $K_{\pm 1/2}$ is the same with far-field of quantum vortex [66] as a topological soliton. In this aspect, is suggestive the energy relaxation and self-organization of plasma in which topological change in \mathbf{R}^3 owing to magnetic reconnection [67, 68] is known to play a leading rôle (e.g., [23]). Specifically, the complexity of a column magnetofluid is expected to be in on our geometrical development. The detailed numerical studies reveal that the relaxation takes place typically in two steps [69, 70]; the first establishes a quasi-equilibrium configuration dominated by a direct current mode (uniform in Z -axis), and the second, the helical configuration as the energy minimum state. In reference to this, we make a heuristic analogy between the former (latter) configuration and the internal harmonic field limited (not limited) to $k \rightarrow 0$. Along with this, we consider the internal topological change that can be decomposed into two processes: (A') the (complex-)homeomorphic and (B') heteromorphic transformation as the representation of (A) and (B), respectively.

For (A'), we make a simple attempt at transforming the elliptic partial differential equation for ϕ into a hyperbolic one, on the base. Practically, this can be performed by the transformation form of $k(= 0) \rightarrow -i\mu^*$ with m unchanged. When it is applied to $\eta \sim I_{\pm 1}(kr)$, which must be, at $r \rightarrow \infty$, internally coexisting with the $K_{\pm 1/2}(kr)$, we have $I_{\pm 1}(kr) \rightarrow \mp iJ_{\pm 1}(\mu^*r)$, where the double signs correspond; this can be interpreted as an internal representation of gauge field transformation. The equation that $\eta(\mu^*r)$ obeys is then given by $(\mu^{*-2}\nabla_{\perp}^2 + 1)\eta = 0$, where $\mu^* \neq 0$. The function η is included in the scalar function $\phi = \eta(\mu^*r)e^{i(\pm\theta - kz)}$ as a solution of the following equation in the cylindrical system:

$$(\Delta + k^2 + \mu^{*2})\phi(r, \theta, z) = 0. \quad (29)$$

Here, k is newly introduced of which the value can be taken arbitrarily. Finite value of k is indicative of onset of the well-defined $\hat{\mathbf{z}} (= \mathbf{k}/k)$. Especially for

$k = 0$, η represents single-valued amplitude of vibration of a circular membrane on z -constant slices. In the current context, regarding $\eta^{g_0}(\mu^*r)$ as the internal potential that acts on $\ell\bar{\ell}$ pair, it is appropriate to interpret the ϕ as a possible representation of internal scalar field of the weak boson; $\|m\| = 1$ and μ^* could be reflected in the spin and mass, respectively (the extended argument is given later in Sect. 6).

In the region that allows for $\xi := \mu^*r (= 0 \cdot \infty^{(l)})$, $\eta \sim \mp i J_{\pm 1}(\xi)$ can be expressed as $-i[J_{-1/2}(\xi) - J_{1/2}(\xi)]/\sqrt{2}$, where $\xi \notin \{0, \infty\}$ is redefined in the transformed system of $m = \pm 1/2$. As concerns coupling of the virtual boson with leptons, we see that modules including the spherical Bessel functions $J_{\mp 1/2}$ are generated by applying $k (= 0) \rightarrow -i\mu$ to the internal pion field. That is, we have $K_{\mp 1/2}(kr) \rightarrow (i\pi/2)e^{\mp i\pi/4}H_{\mp 1/2}^{(1)}(\mu r)$ for the reaction (17), where

$$H_{-1/2}^{(1)}e^{-i\theta/2} = [J_{-1/2}(\mu r) + iJ_{1/2}(\mu r)]e^{-i\theta/2}, \quad (30a)$$

$$iH_{1/2}^{(1)}e^{i\theta/2} = [J_{-1/2}(\mu r) + iJ_{1/2}(\mu r)]e^{i\theta/2}, \quad (30b)$$

and the complex conjugates are

$$\left(H_{-1/2}^{(1)}\right)^* e^{i\theta/2} = [J_{-1/2}(\mu r) - iJ_{1/2}(\mu r)]e^{i\theta/2}, \quad (30c)$$

$$\left(iH_{1/2}^{(1)}\right)^* e^{-i\theta/2} = [J_{-1/2}(\mu r) - iJ_{1/2}(\mu r)]e^{-i\theta/2}, \quad (30d)$$

respectively. Here, $\|m\| = 1/2$ is compared to spin of leptons, and all terms should be multiplied by e^{-ikz} with k newly introduced (as before). The representation with $k = 0$ is compared to rest state of them, whereas $k \neq 0$ to the moving state. For the case in which $k \neq 0$, hereafter we set to as $k > 0$ without loss of generality.

When interpreting (30a) \rightleftharpoons (30c) and (30b) \rightleftharpoons (30d) as the CP transformation operation, we can associate (30a) and (30b) with e_L^- and $(\bar{\nu}_e)_R$, respectively, emitted in the β^- -decay, and (30c) and (30d) with e_R^+ and $(\nu_e)_L$, respectively, in the β^+ -decay. An asymptotic form of radially outgoing s-wave function can be obtained by applying $\mu r (= 0 \cdot \infty^{(l)}) \rightarrow g_0^{-1}\bar{\mu}R$ to $(H_{-1/2}^{(1)})^{g_0}$, that is, $(2/\pi)e^{2i\mu r}/\mu r \rightarrow \sim e^{i\bar{\mu}R}/\bar{\mu}R$, where $\bar{\mu} = [\beta m_e c/\hbar]_{\beta \rightarrow 0}$ stands for the observed wavenumber of nonrelativistic electron. For internal coupling of matter with gauge field, we require $\xi (= \mu^*r) = \mu r$ on the cylindrical base. Here, we redefine ϕ as a module of $\phi_{m'} J_{m'}(\xi)e^{i(m\theta - \mathbf{k}\cdot\mathbf{z})}$, where $m' = \pm m$, and $\phi_{m'}$ is constant fixed later. For $m' = \pm 1/2$, note that $J_{-1/2} \gg J_{1/2}$ for $\mu^* \rightarrow 0$. Wherein the Coulomb potential energy $V(R)$ can be obtained by applying $\xi := \mu^*r (= 0^{(l)} \cdot \infty) \rightarrow g_0^{-1}\bar{\mu}^*R$ to $\|\phi(m' = -1/2)\|^{g_0}$, that is, $\sim \phi_{-1/2}^2/2\xi \rightarrow \alpha/\bar{\mu}^*R =: V(R)/m_e c^2$, with $\phi_{-1/2}^2 \rightarrow \alpha$ and $\bar{\mu}^* = m_e c/\hbar$ (cf. Sect. 3.2). Therefore, $\phi(m' = -1/2)$ can be associated with internal scalar field of the virtual photon concomitant with charged leptons; the $\mu^* \rightarrow 0$ leading the indetermination, with the massless state.

While the process (A') is requisite for the (B'), the latter is to concur with the former. The problem herein is that the (B') should complete the excitation of electron involving the connections among its spatial motion, spin, and photon. For this, there are well-established answers in the form based on the Dirac and Maxwell/Proca wave equations [71]. That is, these equations capture the connections in a way that is impossible using scalar fields, leading to experimental predictions that have precisely been verified. This circumstance stimulates us to geometrically extend, via the (B'), the foregoing scalar form, reducing the second order of derivative to the first one [72]. The extension should be accomplished in such a way that the geometric framework self-contains the scalar form reflected in the lowest energy excitation of the elementary particles. In the scalar one, ϕ satisfies

$$(\Delta + \kappa^2) \phi = 0, \quad (31a)$$

$$\kappa^2 = \mathbf{k}^2 + \mu^{*2}, \quad (31b)$$

and (30) with ξ replacing μr likewise. Regarding the onset of $\hat{\mathbf{z}}$, here we introduce the vector field Φ transformed from ϕ as follows:

$$\Phi(\mathbf{r}) = (\mu^*)^{-2} [\nabla \times \nabla \times (\phi \hat{\mathbf{z}}) + \kappa \nabla \times (\phi \hat{\mathbf{z}})]. \quad (32)$$

This is the solution of

$$\nabla \times \Phi = \kappa \Phi, \quad (33)$$

as far as ϕ satisfies (31) [73]. The field Φ is identical with the Gromeka-Beltrami flow, which is known as representation of force-free magnetic field (proportional to current) of a plasma in \mathbf{R}^3 space. It is noted that in the ideal magnetohydrodynamics in which electric conductivity is assumed to be infinite, the form as with (33), $\nabla \times \mathbf{B} = \lambda \mathbf{B}$ with λ being constant, has been derived from variation of the magnetic energy $\mathcal{H} = \frac{1}{2} \int \|\mathbf{B}\|^2 dV$ under the constraint that the magnetic helicity $\mathcal{H} = \frac{1}{2} \int \mathbf{B} \cdot [(\nabla \times)^{-1} \mathbf{B}] dV$ is invariant, that is, $\delta \mathcal{H} = 0 = \delta \mathcal{H} - \lambda \delta \mathcal{H}$ [22, 23].

Equation (33) can be recognized as the rotational eigenvalue equation [74], so that Φ is referred to as rotational field. In the case for which m is arbitrary, the function of Φ is written out below; this exemplifies generalization of the special case $m = m' = 0$ or ± 1 that the classical field theory often refers to. Substituting $\phi = \phi_{m'} J_{m'}(\xi) e^{i(m\theta - kz)}$ into (32), we obtain the expression of $\Phi = (\Phi_r, \Phi_\theta, \Phi_z)$, where

$$\Phi_r = i \frac{\phi_{m'}}{\mu^*} \left[\frac{m\kappa}{\xi} J_{m'}(\xi) - k \frac{dJ_{m'}(\xi)}{d\xi} \right] e^{i(m\theta - kz)}, \quad (34a)$$

$$\Phi_\theta = \frac{\phi_{m'}}{\mu^*} \left[\frac{m\kappa}{\xi} J_{m'}(\xi) - \kappa \frac{dJ_{m'}(\xi)}{d\xi} \right] e^{i(m\theta - kz)}, \quad (34b)$$

$$\Phi_z = \phi_{m'} J_{m'}(\xi) e^{i(m\theta - kz)}, \quad (34c)$$

and $\xi \notin \{0, \infty\}$. The helical pattern of Φ having rotational and translational symmetry is characterized by m as modal number and k (e.g., see [70] and the references, for the vivid analogy of the classical field). In particular, $\Phi(m = \pm 1/2, m' = \pm 1/2, k)$ can be involved in (30) via $\Phi_z = \phi$ with μr replacing ξ so that the Φ with $\mu^* = \mu$ could serve as building blocks (internal structure, in part) of spin 1/2 point particles. For an eigenflow of Φ , the corresponding eigenvalue of ξ is expected to indicate the mass as the Casimir invariant of the Poincaré group. As the observed mass results from the renormalization, we have a reasoning that the geometric extension could capture the interaction with covariant photons.

4.2 Eigenflows of the Rotational Field

Let us suppose interaction of the *single* particle with gauge fields to be represented as the process in which the internal structure of the particle refers to the eigenflows of Φ , to be regulated. In general, it is known that eigenvalues of the flows are not discrete, spanning total complex plane, when the harmonic field is taken into account [75]. The situation considered here falls under the case in which κ is real, provided ξ and k are real. For seeking the specific solution, from the correspondence of Φ to \mathbf{B} follows: the eigenvalue problem of (33) could be formally compared to the aforementioned problem to find the stationary point, at which \mathbf{B} -field configuration minimizing \mathcal{H} is characterized by the minimum eigenvalue of $\lambda (= \mathcal{H}/\mathcal{K})$. The nontrivial real-value of λ is determined by a condition for magnetic flux; the perfectly conducting wall confining the flux makes the λ -value discrete for the cylindrical mode of $m = \pm 1$. With these in mind, we suppose the internal Hamiltonian with $\|\Phi(m, m')\|^{g_0}$ being the integrand, and that the lowest energy excitation of the spinning particles refers to, for the common m and $m' (= \pm m)$, the eigenvalue of κ whose magnitude is minimum (cf. the pion excitation as the Nambu-Goldstone mode). In determining the value, we impose on Φ the boundary condition of $\Phi_r(r = a) = 0$, which can be expressed as

$$\frac{m\kappa}{\tilde{\xi}} J_{m'}(\tilde{\xi}) - k \left[\frac{dJ_{m'}(\xi)}{d\xi} \right]_{\xi=\tilde{\xi}} = 0, \quad (35)$$

where $\tilde{\xi} = \mu^* a$, and physical meaning of a is clarified later. The root of equation (35) can provide an upper limit of ξ , as the \tilde{k} in Sect. 3.1 does likewise to internally regulate the orbital motion (confinement) of $q\bar{q}$ in the closed \mathbf{R}^3 space. A well-defined domain can then be set in $\xi \geq 0$, excluding the infinity, as compatible with asymptotic property of the harmonic field in the *internal* space. The infinity is called for a specific purpose (cf. Sect. 5.2.1).

In the current context, it is natural to consider that the eigenflows of $\Phi(m = \pm 1/2, m')$ and $\Phi(m = \pm 1, m')$ involving discrete eigenvalues derived from (35) determine electromagnetic and weak susceptibility to the spin 1/2 point particles that are themselves with the non-discrete $\Phi(m = \pm 1/2, m')$ with $\mu^* = \mu$. For example, the eigenflow of $\Phi(m = m' = -1/2)$ is considered

to internally regulate the orbital motion of a charged ℓ_L interacting with electromagnetic field, in parallel to the foregoing quark picture. In the following, we examine the eigenfunctions of $\Phi(m = \pm 1/2, m')$ for $m' = \pm 1/2$ each.

4.2.1 The Case of $m' = 1/2$

Equation (35) for $(m, m') = (1/2, 1/2)$ can be expressed as

$$\tilde{\kappa} + \tilde{k} \left(1 - 2\tilde{\xi} \cot \tilde{\xi} \right) = 0. \quad (36)$$

Here, $\tilde{\kappa} = \kappa a$ and $\tilde{k} = ka$ are real, and we have the relation of $\tilde{\kappa} = \pm \sqrt{\tilde{k}^2 + \tilde{\xi}^2}$ from (31b). Although the root property of (35) depends on the sign of $m\kappa$, rather than κ , the case analysis for the sign of κ each is carried out for given m , for an explanation.

For $\tilde{\kappa} > 0$

We express $\tilde{\kappa}$ as a function of $\tilde{\xi}$, eliminating \tilde{k} , and write the positive $\tilde{\kappa}(\tilde{\xi})$ as $\kappa_R^{(+)}$, where the subscript R stands for right-handedness of the helix ($m > 0$). That is, we have

$$\kappa_R^{(+)} = \frac{\tilde{\xi} \left(2\tilde{\xi} \cot \tilde{\xi} - 1 \right)}{\sqrt{\left(2\tilde{\xi} \cot \tilde{\xi} - 1 \right)^2 - 1}}, \quad (37)$$

valid for $\tilde{\xi} \cot \tilde{\xi} > 1$. In the discrete domains of definition, we investigate existence of the minimum of $\kappa_R^{(+)}$. If there exists, we evaluate $\kappa_R^{(+)} = \tilde{\kappa}$, $\tilde{\xi}$, and $\tilde{k} = \sqrt{\tilde{\kappa}^2 - \tilde{\xi}^2}$ at the stable point: these constitute a set of the eigenvalues for the eigenfunction of Φ . Along this guideline, the function of $\kappa_R^{(+)}(\tilde{\xi})$ is plotted in Fig. 2(a). It is noted that the root space should be restricted to a finite range, as consistent with the finiteness of ξ . Anyhow, we see that there is no local minimum in the domains. It is thus concluded that for $(m, m', \kappa) = (1/2, 1/2, +)$ exists no eigenstate.

For $\tilde{\kappa} < 0$

For (36), $-\tilde{\kappa}$ is expressed as a function of $\tilde{\xi}$, and the positive $-\tilde{\kappa}(\tilde{\xi})$ is denoted as $\kappa_R^{(-)}$; that is,

$$\kappa_R^{(-)} = -\kappa_R^{(+)}, \quad (38)$$

for $\cot \tilde{\xi} < 0$. In Fig. 2(b), the function of $\kappa_R^{(-)}$ is plotted; now we find the local minima in the discrete domains. The equality $d\kappa_R^{(-)}(\tilde{\xi})/d\tilde{\xi} = 0$ provides the eigenvalue equation for $\tilde{\xi}$, which can be expressed as

$$(\tau - 4v^{-1}) (\tau - v^{-1}) v^{-1} + \tau = 0, \quad (39)$$

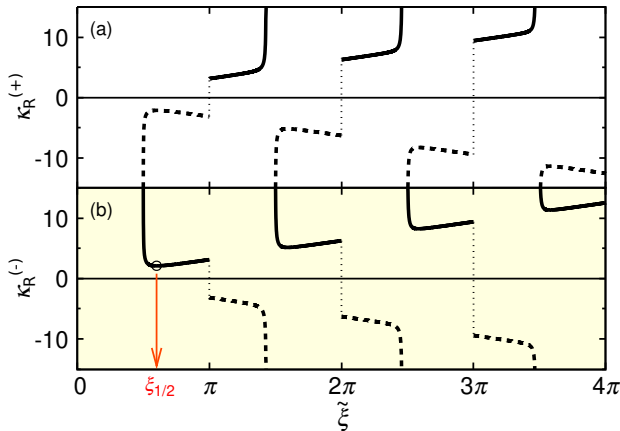


Fig. 2 Plots of $\kappa_{\text{R}}^{(+)}(\tilde{\xi})$ [equation (37)] (a) and $\kappa_{\text{R}}^{(-)}(\tilde{\xi})$ [equation (38)] (b). The functions positive in the discrete domains are shown by the solid curves. Both the figures have a common horizontal axis. In (b), the point at which $\kappa_{\text{R}}^{(-)}$ takes the minimum is indicated by the open circle.

for $v^{-1} < 0$, where $\tau = \tilde{\xi}^{-1}$ and $v = \tan \tilde{\xi}$. The minimum root of (39) is denoted as $\xi_{1/2}$, where the subscript indicates the m' -value. Choosing the minimum value among the local minimum values guarantees the foregoing restriction of root space. It follows that the well-defined $\kappa_{1/2} = \kappa_{\text{R}}^{(-)}(\tilde{\xi} = \xi_{1/2})$ and $k_{1/2} = \sqrt{\kappa_{1/2}^2 - \xi_{1/2}^2}$ are evaluated, to give the rotational eigenvalue of $-\kappa_{1/2}(\xi_{1/2}, k_{1/2})$. This means that, even for the previous case in which $\kappa > 0$, we could have the eigenvalue of $\kappa_{1/2}(\xi_{1/2}, k_{1/2})$ by the change of $m = 1/2 \rightarrow -1/2$, i.e., $(m, m', \kappa) = (-1/2, 1/2, +)$. The values of $\xi_{1/2}$, $\kappa_{1/2}$, and $k_{1/2}$ are listed in the upper row of Table 1.

4.2.2 The Case of $m' = -1/2$

Equation (35) for $(m, m') = (-1/2, -1/2)$ can be expressed as

$$\tilde{\kappa} - \tilde{k} \left(1 + 2\tilde{\xi} \tan \tilde{\xi} \right) = 0. \quad (40)$$

By the method explained above, we look for the eigenvalues the (40) contains.

Table 1 A set of the discrete eigenvalues $\xi_{m'}$, $\kappa_{m'}$, and $k_{m'}$ for $m' = \pm 1/2$.

m'	$\xi_{m'}$	$\kappa_{m'}$	$k_{m'}$
1/2	1.891	2.110	0.9363
-1/2	3.445	3.632	1.152

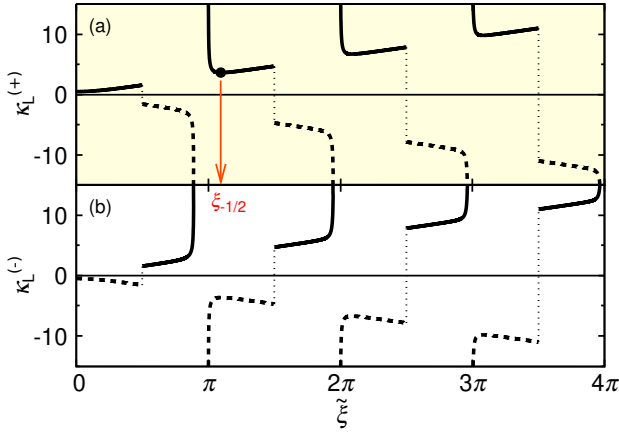


Fig. 3 Plots of $\kappa_L^{(+)}(\tilde{\xi})$ [equation (41)] (a) and $\kappa_L^{(-)}(\tilde{\xi})$ (b). The functions positive in the discrete domains are shown by the solid curves. Both the figures have a common horizontal axis. In (a), the point at which $\kappa_L^{(+)}$ takes the minimum is indicated by the filled circle.

For $\tilde{\kappa} > 0$

For (40), we express $\tilde{\kappa}$ as a function of $\tilde{\xi}$, eliminating \tilde{k} , and write the positive $\tilde{\kappa}(\tilde{\xi})$ as $\kappa_L^{(+)}$, where the subscript L stands for left-handedness of the helix ($m < 0$). That is, we have

$$\kappa_L^{(+)} = \frac{\tilde{\xi} \left(2\tilde{\xi} \tan \tilde{\xi} + 1 \right)}{\sqrt{\left(2\tilde{\xi} \tan \tilde{\xi} + 1 \right)^2 - 1}}, \quad (41)$$

valid for $\tan \tilde{\xi} > 0$. If there exists the minimum of $\kappa_L^{(+)}$ in the domain of definition, $\kappa_L^{(+)} = \tilde{\kappa}$, $\tilde{\xi}$, and \tilde{k} are evaluated at the stable point. In Fig. 3(a), the function of $\kappa_L^{(+)}$ is plotted, to show the profile similar to that displayed in Fig. 2(b), and existence of the local minima in the discrete domains. The equality $d\kappa_L^{(+)}(\tilde{\xi})/d\tilde{\xi} = 0$ provides

$$(\tau + 4v)(\tau + v)v - \tau = 0, \quad (42)$$

for $v > 0$. The minimum root of (42) is denoted as $\tilde{\xi} = \xi_{-1/2}$, which determines the values of $\kappa_{-1/2} = \kappa_L^{(+)}(\tilde{\xi} = \xi_{-1/2})$ and $k_{-1/2} = \sqrt{\kappa_{-1/2}^2 - \xi_{-1/2}^2}$, to give $\kappa_{-1/2}(\xi_{-1/2}, k_{-1/2})$. These values are listed in the bottom row of Table 1.

For $\tilde{\kappa} < 0$

For (40), $-\tilde{\kappa}$ is expressed as a function of $\tilde{\xi}$, and the positive $-\tilde{\kappa}(\tilde{\xi})$ is denoted as $\kappa_L^{(-)}$. The function of $\kappa_L^{(-)} = -\kappa_L^{(+)}$, valid for $\tilde{\xi} \tan \tilde{\xi} < -1$, is plotted in

Table 2 Summary of the rotational eigenvalues.

m	m'	$\kappa (> 0)$	$\kappa (< 0)$	reference ³
m' (L)	$-1/2$	$\kappa_{-1/2}$	—	(30a)
m' (R)	$+1/2$	—	$-\kappa_{1/2}$	(30b)
$-m'$ (R)	$-1/2$	—	$-\kappa_{-1/2}$	(30c)
$-m'$ (L)	$+1/2$	$\kappa_{1/2}$	—	(30d)

³Equation numbers for the leptonic states that refer to the eigenvalues.

Fig. 3(b). As expected, there is no local minimum in the domains: no eigenstate in this case. And yet, by the change of $m = -1/2 \rightarrow 1/2$, i.e., $(m, m', \kappa) = (1/2, -1/2, -)$, we could have $-\kappa_{-1/2}(\xi_{-1/2}, k_{-1/2})$.

4.3 Chiral Asymmetry of the Helical Eigenflows and a Representation of Beta-Decay Products

In light of the allowed combinations of $(m, m', \kappa) = (\pm, \pm, \pm)$, the rotational eigenvalues for $m = \pm 1/2$ are summarized in Table 2. It is proclaimed that the eigenstates do exist for $m\kappa < 0$, whereas do not for $m\kappa > 0$. For the former, Φ_z of the eigenflows for $(m, m', \kappa) = (-, -, +)$, $(+, +, -)$, $(+, -, -)$, and $(-, +, +)$ responds to the term of $J_{-1/2}e^{-i\theta/2}$ in (30a), $iJ_{1/2}e^{i\theta/2}$ (30b), $J_{-1/2}e^{i\theta/2}$ (30c), and $-iJ_{1/2}e^{-i\theta/2}$ (30d), respectively, with $\xi = \mu r$ on the common cylindrical base. For the latter, Φ_z of the non-eigenflows for $(m, m', \kappa) = (-, -, -)$, $(+, +, +)$, $(+, -, +)$, and $(-, +, -)$ responds to $J_{-1/2}e^{-i\theta/2}$ in (30d), $-iJ_{1/2}e^{i\theta/2}$ (30c), $J_{-1/2}e^{i\theta/2}$ (30b), and $iJ_{1/2}e^{-i\theta/2}$ (30a), respectively. Lepton doublet transition in the β^- -decay: $(\nu_e)_L \rightarrow e_L^-$ can be compared to transition of $\kappa_{1/2} \rightarrow \kappa_{-1/2}$ for $(m, \kappa) = (-, +)$, while $(\bar{\nu}_e)_R \rightarrow e_R^+$ in the β^+ -decay, to $-\kappa_{1/2} \rightarrow -\kappa_{-1/2}$ for $(m, \kappa) = (+, -)$. The CP transformation can be seen as the flip of $(m, \kappa) = (-, +) \rightleftharpoons (+, -)$ for m' unchanged.

We now see that, for the reaction (17), ℓ_L and $(\bar{\ell})_R$ must internally refer to the eigenflows of $\Phi(m = -1/2, m' = \mp 1/2, \tilde{\kappa} = \kappa_{\mp 1/2})$ and $\Phi(1/2, \pm 1/2, -\kappa_{\pm 1/2})$, respectively; in particular, charged ℓ_L and neutral $(\bar{\ell})_R$, to $\Phi(m = m' = -1/2, \kappa_{-1/2})$ and $\Phi(m = m' = 1/2, -\kappa_{1/2})$, respectively. Noteworthy is the relation of $\kappa_{-1/2} \neq \kappa_{1/2}$, and chiral asymmetry between L- and R-helix of the eigenflows. This asymmetry is amenable to left-handed selectivity of the charged current weak interaction. According to these ingredients, I put forth the module representation of

$$\Phi\left(-\frac{1}{2}, -\frac{1}{2}, +\right) + i\Phi\left(-\frac{1}{2}, \frac{1}{2}, -\right) =: \Psi_-, \quad (43a)$$

$$\Phi\left(\frac{1}{2}, -\frac{1}{2}, +\right) + i\Phi\left(\frac{1}{2}, \frac{1}{2}, -\right) =: \Psi_+, \quad (43b)$$

for respectively the charged ℓ_L and neutral $(\bar{\ell})_R$ created in the (17). Here, the second and first term in (43a) and (43b), respectively, stand for the orthogonal counterpart having the inverted m' and κ , with respect to $\Phi(m, m', \kappa)$, so that

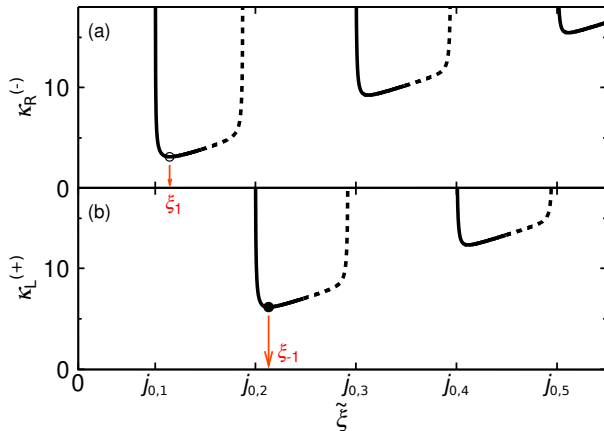


Fig. 4 Plots of $\kappa_R^{(-)}(\tilde{\xi})$ [equation (44)] (a) and $\kappa_L^{(+)}(\tilde{\xi}) = -\kappa_R^{(-)}(\tilde{\xi})$ (b). These functions having, respectively, the domain of $j_{0,n} < \tilde{\xi} < j_{1,n}$ for odd and even number of $n (= 1, 2, 3, \dots)$ are shown by the solid curves. Both the figures have a common horizontal axis, on which positions of $j_{0,n}$ are indicated, in place of scale of the linear axis. The points at which $\kappa_R^{(-)}$ and $\kappa_L^{(+)}$ take the minima in their domains are indicated by the open and the filled circle, respectively. The broken curves in (a,b) correspond to $\kappa_L^{(-)}$ and $\kappa_R^{(+)}$ for $j_{1,n} < \tilde{\xi} < j_{2,n}$ with n odd and even, respectively (see text).

$m\kappa > 0$. The expression of Ψ_{\mp} , i.e., the superposition of the non-discrete flows with $\mu^* = \mu$ can suitably configure (30a) and (30b), respectively. Provided the indication of the lepton mass of $\xi_{\mp 1/2} \rightarrow m_{\ell, \bar{\ell}}$ (cf. Sect. 6.2), $\Psi_{\mp}(\mu, k, \|m\|)$ can be compared to the irreducible representation of the Poincaré group [33]: the free-particle states $|m_{\ell, \bar{\ell}}, p, s\rangle$, where $p = \|\mathbf{P}\|$, and $s = 1/2$ denotes the spin quantum number in $\mathbf{S}^2 = s(s+1)\hbar^2$.

4.4 Remarks on the Integer Modes

For $m = \pm 1$, we outline the results, in that the eigenflows are related to gauge bosons with the spin $\|m\|$. One can calculate the discrete eigenvalues basically along the procedure described above. However, we have only to examine the case of $m = m'$, as $J_{m'}$ and $J_{-m'}$ with m' integer are linearly dependent.

In general, on pattern of existence of the eigenstates, it is found that $\kappa_R^{(-)} (= -\tilde{\kappa} > 0)$ and $\kappa_L^{(+)} (= \tilde{\kappa} > 0)$ with respectively $(m, \kappa) = (+, -)$ and $(-, +)$, i.e., $m\kappa < 0$, have local minima in their domains. As is, a triad of the well-defined eigenvalues ξ_m , κ_m , and k_m can be obtained. For the mode in which m is an even number, we have $\xi_m = \xi_{-m}$, $\kappa_m = \kappa_{-m}$, and $k_m = k_{-m}$, whereas the odd mode provides $\xi_{\|m\|} < \xi_{-\|m\|}$, $\kappa_{\|m\|} < \kappa_{-\|m\|}$, and $k_{\|m\|} < k_{-\|m\|}$ (like for $m = \pm 1/2$), breaking chiral symmetry. This modal parity stems from the relation of $J_{-m} = (-1)^m J_m$. In the special case of $m = 0$, spectrum of $\tilde{\kappa}$ is continuous.

For $m = \pm 1$ of particular interest, the function of $\kappa_{\text{R}}^{(-)}(\tilde{\xi})$ is expressed as

$$\kappa_{\text{R}}^{(-)} = -\frac{\tilde{\xi} \left[\tilde{\xi} J_0(\tilde{\xi}) - J_1(\tilde{\xi}) \right]}{\sqrt{\tilde{\xi} J_0(\tilde{\xi}) \left[\tilde{\xi} J_0(\tilde{\xi}) - 2J_1(\tilde{\xi}) \right]}}, \quad (44)$$

which is related to $\kappa_{\text{L}}^{(+)}(\tilde{\xi})$ as $-\kappa_{\text{R}}^{(-)} = \kappa_{\text{L}}^{(+)}$. Here, the domains of $\kappa_{\text{R}}^{(-)}$ and $\kappa_{\text{L}}^{(+)}$ positive definite are given by $j_{0,n} < \tilde{\xi} < j_{1,n}$ with n being odd and even number, respectively, where $j_{m,n}$ denotes the n -th zero of $J_m(\tilde{\xi})$. The $\kappa_{\text{R}}^{(-)}$ and $\kappa_{\text{L}}^{(+)}$ are plotted in Fig. 4(a,b), respectively. We find the local minima in the domains, and that $\kappa_{\text{L}}^{(-)}$ and $\kappa_{\text{R}}^{(+)}$ with $m\kappa > 0$ have no such points in their domains given by $j_{1,n} < \tilde{\xi} < j_{2,n}$ with n odd and even, respectively. The eigenvalue equation for $\tilde{\xi}$ can be written as

$$J_0^2(\tilde{\xi}) \left[\tilde{\xi} J_0(\tilde{\xi}) - 2J_1(\tilde{\xi}) \right] + J_1^3(\tilde{\xi}) = 0. \quad (45)$$

The roots in $j_{0,1} < \tilde{\xi} < j_{1,1}$ and $j_{0,2} < \tilde{\xi} < j_{1,2}$ are denoted as ξ_1 and ξ_{-1} , respectively; they provide $\kappa_1 = \kappa_{\text{R}}^{(-)}(\tilde{\xi} = \xi_1)$, $\kappa_{-1} = \kappa_{\text{L}}^{(+)}(\tilde{\xi} = \xi_{-1})$, and $k_{\pm 1} = \sqrt{\kappa_{\pm 1}^2 - \xi_{\pm 1}^2}$. For convenience, the values are listed in Table 3.

Table 3 A set of the discrete eigenvalues ξ_m , κ_m , and k_m for $m = \pm 1$.

$m (= m')$	ξ_m	κ_m	k_m
1	2.857	3.112	1.234
-1	5.937	6.162	1.652

5 Observability of the Rotational Field

5.1 Relation of the Field with Nonrelativistic Kinematics of a Fermionic Particle

We consider application of the developed formalism to an observational issue on Ψ_- including the interactive module $\Phi(m = m' = -1/2, \kappa > 0)$. Concerning the operation with $r \rightarrow \infty$, we do not have the constraint on $k \rightarrow 0$ that has been required for the $\|m\| = 1/2$ system of internal pion field to expand as compatible with the $\|m\| = 1$ system. This resembles the situation in which the transformation (24) is applicable to reproduction of the Cornell potential for $q\bar{q}$ moving nonrelativistically. It is, therefore, conceivable that kinematics derived from the Ψ_- for $k \rightarrow 0$ is of the charged ℓ moving nonrelativistically

(i.e., $\beta \rightarrow 0$ and $\bar{\mu} \neq 0$). When $k \rightarrow 0$ is taken for $k \neq 0$ prerequisite to the reference to an eigenflow, the operation can be translated as projection of the helical field onto the cylindrical base. For spatial transformation reflecting it, we invoke the extended form of

$$\kappa \mathbf{r} \longrightarrow \text{sgn}(\kappa) g_0^{-1} \mu \boldsymbol{\rho}, \quad (46)$$

where $\text{sgn}(\kappa \geq 0) = \pm 1$, $\boldsymbol{\rho}$ is radial coordinate vector on a complex plane (with its origin o), and $\mu \|\boldsymbol{\rho}\| = \mu r$.

For kinematic states of a single electron, we see the geometric mechanics that covers SU(2), say, the Lie algebraic representation of $\mathbf{S} = (\hbar/2)\boldsymbol{\sigma}$, where $\boldsymbol{\sigma}$ is the vector of Pauli matrices: $(\sigma_1, \sigma_2, \sigma_3)$ [17]. In the special case of $k = 0$ compared to the rest state, it is trivial that sign of Ψ_- is inverted by the rotation of $\theta = 0 \rightarrow 2\pi$, and recovered first by that of 4π . We render the rotation center o identical with the origin O at which the electron is at rest. When making the rotation angle of either $-\theta$ or θ correspond to \mathbf{R}^2 -rotation angle Θ , therefore, Ψ_- captures a basic property of \mathbf{S} that rotational operator generates $\exp[i\boldsymbol{\Theta} \cdot \mathbf{S}/\hbar]_{\|\boldsymbol{\Theta}\|=2\pi} = -I$, where $\|\boldsymbol{\Theta}\| = \Theta$, and $I (= \sigma_1^2 = \sigma_2^2 = \sigma_3^2)$ is the unit matrix.

For the case of $k \neq 0$, we take account of motion of spin and circular orbit of an electron affected by time-independent uniform magnetic field \mathbf{B} , as shown in Fig. 5(a) (see figure 3-3 in [46], and the relevant explanations therein). The given is a simple situation in which the helicity is conserved, according to the original Dirac's theory: relativistic quantum mechanics. Concerning access to Φ of the nonrelativistic electron, transformation of $kz \rightarrow g_0^{-1}(1 - \delta_g)\bar{\mu}\zeta$, in conjunction with (46), is applied to the phase factor of Φ_z raised to the power of g_0 . Here, μ has been replaced by $(1 - \delta_g)\bar{\mu}$, with δ_g being $1 - \sqrt{1 - \delta} = \delta/2 + \dots$. On the resulting $e^{-i[\theta + (1 - \delta_g)\bar{\mu}\zeta]}$, we impose the lifting shift of $(\theta, \zeta) = (0, 0) \rightarrow (-2\pi, 2\pi\bar{\mu}^{-1})$, which advances the phase. In accordance with the L/R definition for helix, let negative sign of rotational angles be clockwise. Denoting by $\Delta\theta$ the advanced phase, we get $\delta_g = \Delta\theta/2\pi$, which can be compared to radiative correction term in the g -factor of $2[1 + \Delta\Theta/(2\pi\Gamma)]$, where $\Gamma = (1 - \beta^2)^{-1/2}$, and $\Delta\Theta = \Gamma\Delta\Theta(\Gamma \rightarrow 1)$ is the observed advancing angle of spin precession, namely, the Thomas precession. For anti-clockwise, $\Theta (= -\theta) = 2\pi$ rotation of unit coordinate vector $\hat{\mathbf{r}}$ as shown in Fig. 5(b), we find the correspondence between $\Delta\Theta/\Gamma$ and $\Delta\theta$:

$$\Delta\theta \longleftrightarrow \Delta\Theta(\beta \rightarrow 0). \quad (47)$$

Our approach allows for the quantum correction of the pure Dirac particle for which $\Delta\Theta = 0$.

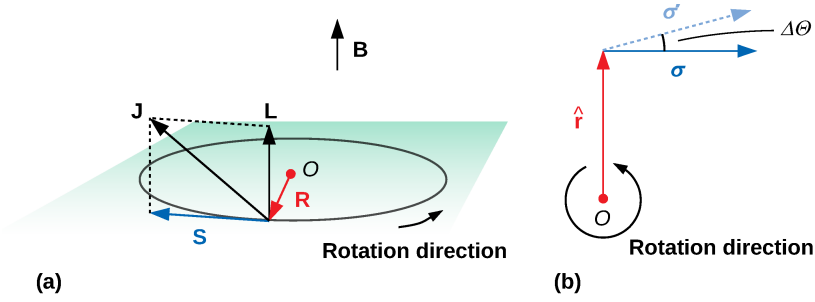


Fig. 5 Cyclotron motion of a single electron having the spin \mathbf{S} and its longitudinally polarized state (a), and the corresponding rotation of unit radial vector $\hat{\mathbf{r}} = \mathbf{R}/\|\mathbf{R}\|$ and change of the polarization for the one orbital turn: $\sigma \rightarrow \sigma'$ (b). In (a), the angular momentum coupling is depicted.

5.2 Internal Mechanism Advancing Spin Precession Frequency

5.2.1 Coordinate Mechanics of the Charged Fermion

The internal mechanics determining the value of $\Delta\theta$ is to respond to the full information of the observed kinematic state, which is contained in the total angular momentum as the coupling of the orbital angular momentum \mathbf{L} and \mathbf{S} (e.g., [18]):

$$\mathbf{J} = \mathbf{L} + \mathbf{S}, \quad (48a)$$

as depicted in Fig. 5(a). We pay attention to the formalism in which the (48a) divided by \hbar , for $\beta \rightarrow 0$, gives

$$\mathbf{J}/\hbar \longrightarrow \mathbf{S}/\hbar. \quad (48b)$$

Reminding this, we find out internal coordinates reflected in the rotational $\hat{\mathbf{r}}$ and σ . By combining the correspondence $\Phi \leftrightarrow \mathbf{B}$ with (3), we prepare the function-space transformation of $\Phi \rightarrow i\tilde{\lambda}\mathbf{r}$, where $\tilde{\lambda}$ is dimensionless real-constant, for its application to equation (33) with μ replacing μ^* . Taking this into account, we introduce the covering vector for $\mathbf{J}/(\hbar\sqrt{3})$, defined by

$$\mathbf{\Lambda} := [\nabla \times \Phi]_{\Phi \rightarrow i\tilde{\lambda}\mathbf{r}} = i\tilde{\lambda}\kappa\mathbf{r}. \quad (49)$$

The terminology of the internal vector is from interpreting the helical Φ as a covering space. Now, the transformation (46) cooperated with $k \rightarrow 0$ is applied to $\mathbf{\Lambda}$. We then have the following form just in parallel with (48b):

$$\mathbf{\Lambda} \longrightarrow \mathbf{\Lambda}_0, \quad (50a)$$

where

$$\mathbf{\Lambda}_0 = \text{sgn}(\kappa) i\tilde{\lambda}g_0^{-1}\mu\rho. \quad (50b)$$

In the context, the quantity $\mathbf{\Lambda}_0$ with $\text{sgn}(\kappa) = +1$ must describe $\mathbf{S}/(\hbar\sqrt{3})$ of the electron moving nonrelativistically; the condition is investigated below. At the outset, we normalize (50b), to provide the following symbolic master equation that spin-half particles are to refer to:

$$\hat{\sigma} = \text{sgn}(\kappa) i\xi\hat{\rho}, \quad (51a)$$

where

$$\hat{\sigma} = \mathbf{\Lambda}_0/(\tilde{\lambda}/g_0), \quad \hat{\rho} = \boldsymbol{\rho}/\|\boldsymbol{\rho}\|, \quad (51b)$$

and $\xi = \mu\|\boldsymbol{\rho}\|$, which connotes coupling of $\mu\|\boldsymbol{\rho}\|$ with $\mu^*r =: \xi$ (Sect. 4.1). Equation (51a) captures orthogonality of the base spaces accommodating $(\boldsymbol{\rho}, \mathbf{\Lambda}_0)$, to serve as the coordinate-rotor. This is expected to rule infinitesimal rotations (in the sense of standard analysis), as intuitively seen by the familiar form: the isomorphism between SU(2) and SO(3) Lie algebra with the generators S_i and X_i , respectively, is sustained via $S_i = i\chi X_i$, where χ is constant that depends on the way of defining the basis vectors.

We delve into realistic rotation of the internal $(\boldsymbol{\rho}, \mathbf{\Lambda}_0)$ for $\text{sgn}(\kappa) = +1$, in terms of self-consistent procedure of the normalization. First, suppose that $\hat{\rho}$ is a basis vector normalized when $\boldsymbol{\rho}$ gets on real axis of the complex plane. Then, trivially $\|\hat{\rho}\| = 1$ is set on the real axis, and the real basis vector is to come out in $\hat{\mathbf{r}}$. The vector configuration of (51a) on this plane is illustrated in Fig. 6(a), providing a value of ξ larger than unity. Second, suppose that $\hat{\sigma}$ is another independent basis vector normalized when $\boldsymbol{\rho}$ rotates by $-\pi/2$ to be purely imaginary and $\mathbf{\Lambda}_0$ gets on the real axis. For $\lambda = 1$, we can identify $\|\mathbf{\Lambda}_0\| = \lambda/g_0$ with $\|\mathbf{S}\|/(\hbar\sqrt{3}) = 1/2$. Then, $\|\hat{\sigma}\| = 1$ is set on the real axis; the vector configuration of (51a) on the second plane is shown in Fig. 6(b). Besides, the vector configuration of $(\hat{\mathbf{r}}, \boldsymbol{\sigma})$ [Fig. 5(b)] is recast to the one of $(\hat{\rho}, \hat{\sigma})$ on a normalized complex plane, which is shown in Fig. 6(c). This can be regarded as superposition of $\hat{\rho}$ on the first plane (a) and $\hat{\sigma}$ put on the imaginary axis by the rotation of $\pi/2$ on the second plane (b). For Θ and θ as rotation angles of $\hat{\mathbf{r}}$ and $\hat{\rho}$, respectively, we have $\Theta = -\theta$, and therefore, $\hat{\rho}$ rotated by -2π is to coincide with the initial one. On the other hand, $\boldsymbol{\sigma} \rightarrow \boldsymbol{\sigma}'$ incidental to the one turn of $\hat{\mathbf{r}}$ should be described by $\hat{\sigma} \rightarrow \hat{\sigma}'$ with $\Delta\theta$, where $\|\hat{\sigma}\| = \|\hat{\sigma}'\| = 1$ is imposed. Then, $\hat{\sigma}$ captures $\boldsymbol{\sigma}/\sqrt{3}$, on account of $\hat{\sigma}^2 \rightarrow \boldsymbol{\sigma}^2/3 = I$. That tips of both the $\hat{\rho}$ and $\hat{\sigma}$ sweep unit circle on the plane (c) represents unitary evolution of Ψ_- , and is necessary for the normalized two-dimensional complex space to be the point: $\hat{\rho} + i\hat{\sigma} = 0$ (cf. Sect. 2.3).

In that regard, the $r \rightarrow \infty$ can be related to setting unit sphere subtracted by a spherical cap except the North pole (namely, the partial Riemann sphere), so as to cover $\mathbb{C}_{*(-1/2)} \cup \{\infty\}$. Here, $\mathbb{C}_{*(m')}$ = $\{\mu\boldsymbol{\rho} \in \mathbb{C} \mid 0 < \mu\|\boldsymbol{\rho}\| < \xi_{m'}\}$; note that its planar shape is similar to that for the Cornell regime. The connection of the complex space to \mathbf{R}^2 , requisite for the observation, is established through the North pole from which to exert stereographic projection of the partial sphere onto $\mathbb{C}_{*(-1/2)}$, and vice versa. As the normalized plane (c) virtually

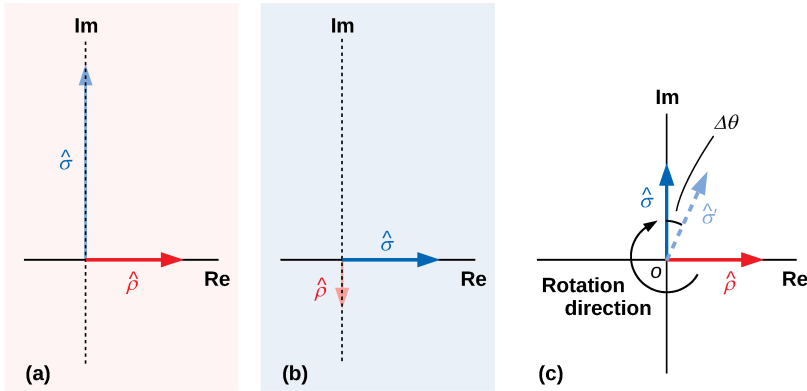


Fig. 6 Complex planes setting, on the real axes, $\|\hat{\rho}\| = 1$ (a) and $\|\hat{\sigma}\| = 1$ (b) for a common ξ -value (> 1), and a normalized complex plane (c) corresponding to Fig. 5(b).

consists of the two leaves (sharing the real axis), the extended set is twofold, allowing for two points at infinity. Orthogonality of the leaves is to prohibit degeneracy of the points, to give the distinct $\{+\infty\}$ and $\{-\infty\}$ that anchor the connection via the real axis.

It turns out, for $\tilde{\lambda}\hat{\sigma} \rightarrow \sigma/\sqrt{3}$, that $\Lambda_0 = (\tilde{\lambda}/g_0)\hat{\sigma}$ is rightly reflected in $\mathbf{S}/(\hbar\sqrt{3})$. Herewith, we see that replacement of $\lambda \rightarrow \hbar$ leads to appearance of minimum action; that is, \mathbf{S}/\hbar turns into small, dimensional operator of \mathbf{S} . This property is compatible with the characteristic of state vector and its unitary evolution, regardless of the value of \hbar itself. Specifically, the $\tilde{\lambda} = 1$ can be interpreted as an internal unit reflected in quantum bit (“qubit”), i.e., the basic unit of quantum information [76]. The relevant issue is important, which includes responsibility of the internal mechanics to the quantum entanglement [77] and measurements of many-body systems [78, 79], but seems to be somewhat out of scope in this paper.

5.2.2 Concept of Coordinate Self-renormalization

It is obvious that $\hat{\rho}$ represents $(n_d - 1)$ -dimensional projective (tangential) plane of \mathbf{r}^{n_d} space having the dimensions of $n_d = 3$, and $\hat{\sigma}$ does likewise. In addition, ξ takes on one degree of freedom that mediates between those two spaces. Although $\hat{\rho}$ and $\hat{\sigma}$ are distinguished from one another, $\hat{\sigma}$ in Fig. 6(b) just embodies $\hat{\rho}$ in (a) on the real axis, so that observer has no way of distinguishing both the basis vectors for the comparison. This suggests the isotopic relation of $\hat{\sigma}$ to $\hat{\rho}$ by which, after the aforementioned clockwise quarter-turn of $\boldsymbol{\rho}$, $\hat{\sigma}$ maintains gauge of the real axis, on behalf of $\hat{\rho}$ that was thereon before the turn. This instant, $\hat{\rho}$ is on the imaginary axis, having the magnitude of $1/\xi$. That is, as seen in Fig. 6(a,b), the turn enforces the shrinkage of $\hat{\rho}$, which is undetectable at this moment. Especially for the one clockwise turn, the vector shrunk up gets again on the real axis, to be expressed as $\Delta\hat{\rho} = (1/\xi^4)\hat{\rho}$. This must be an observable piece. Meanwhile, for the one turn of $\hat{\rho}$ in Fig. 6(c), $\|\hat{\rho}\|$

is to remain unchanged. To reconcile the both, we should consider that the apparent $\hat{\rho}$ having $\|\hat{\rho}\| = 1$ results from superposition of $\Delta\hat{\rho}$ on a coordinative vector provisionally normalized on the real axis in an alternative way. Expected is that the scalar ξ plays a key rôle in the primitive process, referred to as coordinate self-renormalization (CSR), hereafter.

Concerning the pre-normalization, it is reasonable to recall the critical value of ξ , i.e., $\tilde{\xi} = \mu^*a$, to give $\hat{\rho}_a = \boldsymbol{\rho}/a$ having its magnitude of $\xi/\tilde{\xi}$. By employing them, one can rewrite $\xi\hat{\rho}$ as $\tilde{\xi}\hat{\rho}_a$ in (51a). This prescribes the coordinate setup that enables the interactive Φ to refer to an eigenflow. Note here that $\|\hat{\rho}_a\| < \|\hat{\rho}\|$ because of $\xi < \tilde{\xi}$. Taking these into account, we make the following transformation that undertakes the CSR:

$$\hat{\rho}_a \longrightarrow \hat{\rho} = \hat{\rho}_a + \Delta\hat{\rho}, \quad (52)$$

on \mathfrak{R} . For $\Delta\hat{\rho}$ to be observable will require complementation between $\Delta\hat{\rho}$ and $\Delta\theta$, in harmony with the isotopic relation between $\hat{\rho}$ and $\hat{\sigma}$. That is, it is supposed that the transformation of

$$\hat{\sigma} \longrightarrow \hat{\sigma}' = \hat{\sigma} + \Delta\hat{\sigma} \quad (53)$$

is carried out in the way the following relation holds:

$$\Delta\hat{\rho} = \mathfrak{R}(\Delta\hat{\sigma}), \quad (54)$$

as displayed in Fig. 7. The CSR can be regarded as the process that transforms the complex orthogonal superposition of the two isotopic spaces (as consistent with Ψ_-) into the real superposition, without violating the condition for the complex space to be the point.

5.3 Generation of a Numerical Value Comparable to α

From (54), we have $\|\Delta\hat{\rho}\| = \|\hat{\sigma}'\| \sin \Delta\theta$. Equating this to the relation of $\|\Delta\hat{\rho}\| = 1/\xi^4$ yields the equation that connects ξ and $\Delta\theta$:

$$\xi^{-4} = \sin \Delta\theta. \quad (55)$$

Another equation independent of (55) is given by $\xi\|\hat{\rho}\| = \tilde{\xi}\|\hat{\rho}_a\|$ with $\|\hat{\rho}_a\| = 1 - \|\Delta\hat{\rho}\|$. We have the expression of

$$\xi = \xi_{-1/2} (1 - \xi^{-4}), \quad (56)$$

where $\tilde{\xi}$ has been set to the critical value in $\mathbb{C}_{*(-1/2)}$ by which the open set is well defined. The corresponding $r = a$, denoted as $a_{-1/2}$, specifies radius of internal cylinder to confine the field $\Phi(m = m' = -1/2, \kappa > 0)$ and its orthogonal counterpart, as well, by virtue of the consistent coordinate-normalization

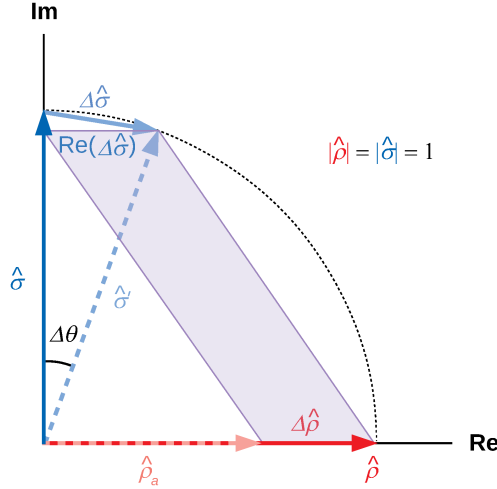


Fig. 7 A schematic to explain how to harmonize the transformation of $\hat{\rho}_a \rightarrow \hat{\rho}$ with $\hat{\sigma} \rightarrow \hat{\sigma}'$. The dotted curve indicates equator of the Riemann sphere.

of the orthogonal space. That is, the gauge-fixing $\tilde{\xi} = \xi_{-1/2}$ enables the eigenflow $\Phi(m = m' = -1/2, \kappa_{-1/2})$ to regulate the Ψ_- , properly connecting ρ with \mathbf{R} . The connection through the infinity, accommodated by the confinement, is to respond to physical (QED) picture of coupling the infinitesimal point charge with the photon field.

In order to highlight the physical correspondence, we approximately solve the set of equations (55) and (56), assuming $\Delta\theta \ll 1$. When ignoring $\sim (\Delta\theta)^3$ and the higher order terms, (55) reduces to

$$\xi^{-4} \cong \Delta\theta, \quad (57)$$

and (56) allows the expression of

$$\xi^{-4} \cong \xi_{-1/2}^{-4} / (1 - 4\xi_{-1/2}^{-4}). \quad (58)$$

Thus, if only the numerical value of $\xi_{-1/2}$ is given (cf. Table 1), one can algebraically calculate the values of ξ and $\Delta\theta$ from (57) and (58). By (57), the correspondence (47) is cast to $\sim \xi^{-4} \leftrightarrow \Delta\theta(\beta \rightarrow 0)$. For the theoretical consistency, the scalar quantity ξ^{-4} must indicate a value comparable to α [80]. Indeed, substituting $\xi_{-1/2}^4 \cong 141$ into (58) leads to $\xi^4 \cong 137$ so that the assumption of $\Delta\theta \ll 1$ is valid. The result suggests that Ψ_- does not only provide the geometric representation as compared to the Wigner's classification, but also be structure, i.e., *physical* reality of the electron. It is noted that the value of ξ^4 is unchanged under the inverse rotation ($m = -m' > 0$) of the coordinate-rotor with $\text{sgn}(\kappa) = -1$ (Sect. 4.3), regulated by the common $\mathbb{C}_{*(-1/2)}$; this property is responsible for the *CP* invariant along with the positron state.

A tick of $\Delta\theta (\leftarrow \Delta\hat{\rho} > 0) = 2\pi\delta_g$ measures out one cyclotron-period independently of electron velocity. We thus see that the scalar correction in the g -factor (the magnetic moment anomaly) can be regarded as the modest appearance of one-dimension of time, which reflects release of the degree of freedom of ξ through the process properly connecting the complex n_d -dimensional space with \mathbf{R}^{n_d} space. It follows from this that dimensions of space-time are $3n_d + 1 = 10$, and conceivable degrees of freedom add up to 11.

The number appears to coincide with that required for unification of the theory having $SU(3) \times SU(2) \times U(1)$ symmetry and gravitational theory, specifically, that as a far-reaching consequence in [81]. Accordingly there is, more or less, a possibility that the current geometry is linked to the one in the string theory. However, it should be noted that a significant difference exists between their background vacua: the field Ψ_- pervades the realistic space beyond the point in \mathbf{R}^3 , and undergoes the cylindrical confinement in $\xi < \xi_{-1/2} \neq \infty$ when regulated. As is, the operational methodology to see the internal landscape through the point (instead of an ingredient having the finite size of $\sim l_P$) is apparently free from the problem of compactification incidental to the higher-dimensional theories extended along Kaluza-Klein theory [82, 83], whereas the stereographic projection corresponds to a class of Alexandroff one-point compactification of the complex space. The causal disconnection of the double vacuum, which accompanies the operation owing to the indeterminate form (Sect. 2.3), is essential for the four-dimensional spatiotemporal setup mentioned above (also, compatible with the quantum measurements). This means that the internal mechanics is not subjected to our space-time; this theory belongs to a category of background-independent theories in the conventional sense.

Along time-energy- $\Delta\hat{\rho}$ correspondence in four vector, the scale of $\sim \xi^{-4}$ can be translated as origin of electric energy of the point charge excited in our vacuum. Then, inequality of $\xi^{-4} > \xi_{-1/2}^{-4}$ is amenable to the QED vacuum picture in which net charge decreases outward due to polarization of virtual electron-positron pairs. Effective thickness of the shielding shell is deemed to reflect $\Delta\xi = \xi_{-1/2} - \xi$. Denoting by e_{th} a finite charge that should theoretically be determined, one has $e^2 = e_{\text{th}}^2/(1 - Y_c)$ with Y_c being constant, in natural units [30]. Now we see the remarkable correspondence between the e^2 -expression and (58); Y_c reflects the quantity of $\sim 4\xi_{-1/2}^{-4}$, to be expressed as $4e_{\text{th}}^2$ approximately.⁴ It is claimed that physical meaning of the charge renormalization, which copes with photon self-energy, can be ascribed to the CSR regulated by a rotational eigenvalue for $m' < 0$.

⁴One can find “ $e_{\text{th}}^2 = 1/141$ ” in a *completely speculative* sentence of Feynman’s lecture note [30].

6 Further Discussions on the Compatibility with the Standard Model

In order to make the theory self-contained, I provide a concise explanation of how the internal mechanics could be linked to an internal representation responsible for the quark and weak charge and leptonic mass that characterize the electron-based β -decay. The argument is expanded in a way we could track its compatibility with the standard model. The manner is reasonable in that the standard model systematically describes almost all experimental results with highest accuracy at present.

6.1 Quark Electric Charge

We attempt to connect the CSR with the representation potentially reflected in the quark electric charge. This is a subject to the electroweak interaction in the closed space confining quarks. In the internal system in which equation (20) with $m = \pm 1$ holds, reconsider the region of $r \rightarrow \infty$ so that the solution can be expressed as $\eta(kr) \sim I_{\pm 1}(kr) \gg K_{\pm 1}(kr)$ (Sect. 4.1). This corresponds to the physical situation in which the low-energy limit is considered far away from the high-energy (perturbative QCD) region characterized by the asymptotic freedom [84, 85]. The internal k -transformation applied to $I_{\pm 1}(kr)$ is recast to the form of

$$kr \longrightarrow \varphi := -i\xi, \quad (59)$$

with $\xi := \mu^* r$. It is supposed that, the process in which $W^{\pm,0}$ and B^0 particles appear is signified by the transformation of $\eta(kr)$ owing to (59). Transformation of the η^{g_0} norm is written as follows:

$$\eta^{g_0}(kr) \longrightarrow U_{\pm}(\xi) = -\phi_{\pm 1}^2 J_{\pm 1}^2(\xi). \quad (60)$$

Equation (60) could represent generation of the internal potential that acts on $\ell\bar{\ell}$ pair separated, in dual relation to the (28) that represents generation of the external potential of $q\bar{q}$ pair confined. For convenience, the function transformation of $I_{\pm 1}(kr) = I_{\pm 1}[(k/\mu^*)\xi] \rightarrow -J_{\pm 1}^2(\xi)$ is shown in Fig. 8. Since $\phi_{\pm 1} J_{\pm 1}(\xi)$ constitutes Φ_z , it is reasonable to suppose that $\Phi(m = m' = \pm 1, \mp \kappa_{\pm 1})$ internally regulates the weak interaction, as the $\Phi(m = m' = -1/2, \kappa_{-1/2})$ regulates the electromagnetic interaction. Henceforth, the eigenflows for which $m = m'$ are denoted as Φ_m .

We focus on the β^- -decay reaction, decomposed into $d_{(-1/2)} \longrightarrow u_{(1/2)} + W_{(-1)}^-$ and $W_{(-1)}^- + \nu_{e(1/2)} \longrightarrow e_{(-1/2)}^-$. Here, the values in the brackets indicate the third component of the weak isospin, T_3 . Along the relation of $\Phi_{-1/2}$ with $e_{(-1/2)}^-$, we make the correspondence between m and T_3 for particle species endowed with negative charge and negative T_3 . The Yukawa interaction is rewritten in the form

$$[d_L + (\bar{u})_R] \longrightarrow W^-, \quad W^- \longrightarrow e_L^- + (\bar{\nu}_e)_R. \quad (61)$$

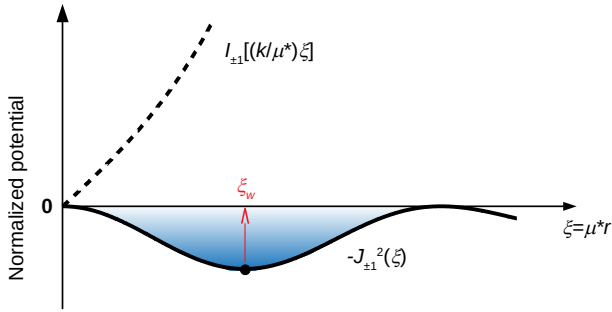


Fig. 8 The transformation of the cylindrical functions, $I_{\pm 1} \rightarrow -J_{\pm 1}^2$, caused by (59). On the horizontal axis, ξ_w denotes the value of ξ at which the resulting function as the normalized potential $U_{\pm}(\xi)/\phi_{\pm 1}^2$ (solid curve) gives a minimum value.

Here, the square bracket emphasizes the fact that the $d\bar{u}$ pair is confined in the closed space of pion interior.

Now we reconsider the charged current interaction of d_L (undergoing rotational motion in the closed space) with W^- . We read that the left-handed d_L , involved in the interaction along with e_L^- , goes for the CSR owing to (51a) with $\text{sgn}(\kappa) = +1$, as basic internal mechanics of $T_3 = -1/2$ [$(\bar{d})_R$ and e_R^+ , (51a) with $\text{sgn}(\kappa) = -1$, as that of $T_3 = 1/2$]. It is seen that for rotational motion of e^- , the CSR referring to $\mathbb{C}_{*(-1/2)}$ sets up a proper rotational coordinate in the \mathbf{R}^3 space that allows the orbit. This setup is none other than development of electromagnetic potential. In this view, is expected that the CSR referring to $\mathbb{C}_{*(-1)}$ contributes to setting up a proper coordinate, i.e., developing the interaction potential, in the closed space of $J^P = 0^-$ particle. In particular, the gauge-fixing $\tilde{\xi} = \xi_{-1}$ must be involved in determining negative charge of the d quark, in the same way as the determination of $-e$ in which $\tilde{\xi} = \xi_{-1/2}$ is involved. In this regime, the $k \rightarrow 0$ as a premise of (51a) is supposed to capture the lowest energy excitation of the pion, instead of relativistic excitation of the constituent quarks.

From this notion follows: the ξ^{-4} -scale of (58) with ξ_{-1} replacing $\xi_{-1/2}$ must be responsible for square of the d quark charge $-e_q$. This replacement owes to base coupling between $\Phi_{-1/2}$ and Φ_{-1} via ξ . As a consequence, we have the following expression compared to $\sqrt{e_q^2/e^2} = 1/3$ [41]:

$$\sqrt{(\xi_{-1/2}^4 - 4)/(\xi_{-1}^4 - 4)} \cong 0.333, \quad (62)$$

where use has been made of $\xi_{-1}^4 \cong 1240$ (Table 3). The outcome indicates the overall consistency with the quark model relying on SU(3) symmetry, supporting the relevance of the potential theory that has preliminarily been developed in Sect. 3.

6.2 Vacuum and Mass Generation

We further examine the transformation of (60), in terms of the mass change $m_W \rightarrow m_{\ell, \bar{\ell}}$ in the second equation of (61). By the transformation, the value of ξ at which the potential indicates the minimum changes from 0 to $\xi_w \neq 0$, as seen in Fig. 8. The value of ξ_w characterizes the quantity μ^* included in Φ_{-1} , so that ξ_w must be reflected in m_W .

For real ξ , expansion of $J_{\pm 1}^2(\xi)$ can be expressed as a function of $\xi^2 = \varphi^* \varphi$, where the asterisk signifies the complex conjugate. Accordingly, we have

$$U_{\pm}(\varphi^* \varphi) = -\frac{\phi_{\pm 1}^2}{4} \left[\varphi^* \varphi - \frac{1}{4}(\varphi^* \varphi)^2 + \mathcal{O}((\varphi^* \varphi)^3) \right]. \quad (63)$$

For a comparison, we shall call the standard vacuum model [42], in which one assumes condensate of complex scalar field (denoted as φ'). Potential energy(-density) of the self-interacting φ' is written in the approximate form of $U(\varphi'^* \varphi') \cong \mu^2 \varphi'^* \varphi' + \lambda (\varphi'^* \varphi')^2$, where μ^2 and λ are constants. Vacuum state is represented by the expectation value of φ' , such as $\langle \varphi' \rangle_0 = 0$ for $\mu^2 > 0$: the value of $\sqrt{\varphi'^* \varphi'}$ at which U indicates the minimum. As for $\mu^2 < 0$, it is found that U indicates the minimum at $\varphi'^* \varphi' = -\mu^2/2\lambda$, to give $\langle \varphi' \rangle_0 = \sqrt{-\mu^2/2\lambda}$, which linearly couples with m_W . Quantum excitation of the field can be expressed as $\varphi' = \langle \varphi' \rangle_0 + H/\sqrt{2}$, where H the Higgs boson. Apparently, the analytic function of $U_{\pm}(\varphi^* \varphi)$ is compatible with $U(\varphi'^* \varphi')$ for $\mu^2 < 0$. Provided that $\varphi'^* \varphi'$ in our space-time reflects $\varphi^* \varphi$, thus, we have

$$\sqrt{\varphi^* \varphi} = \xi_w \longleftrightarrow \langle \varphi' \rangle_0, \quad (64)$$

which supports the relation of $\xi_w \propto m_W$. The transformation (59) and the definite onset of $\hat{\mathbf{z}}$ are found to be requisite for generating ξ_w .

In connection with the chiral asymmetry of $\Phi_{\pm \| m \|}$, recall that $(\bar{\nu}_e)_R$ is to internally refer to $\Phi_{1/2}$. The natural extension leads to the idea that the spin 1 neutral boson that can interact with right-handed particles, namely B^0 , refers to Φ_1 . For the eigenvalue, in keeping with what ξ_{-1} contributes to determining e_q of the $J^P = 0^-$ particle, we conjecture that its counterpart, ξ_1 , indicates mass of 0^+ particle, specifically, the Higgs boson mass m_H . The point is that, provided a pair of $\Phi_{\pm 1}$ shares the same base coordinate with the common variable a , the ratio ξ_1/ξ_w must be reflected in mass ratio of m_H/m_W . The specific values of $\xi_1 \cong 2.86$ and $\xi_w \cong 1.84$ give $\xi_1/\xi_w \cong 1.55$. This indeed accords with $m_H/m_W \cong 1.55$ for the experimental values of $m_W \cong 80.4 \text{ GeV}/c^2$ [9, 86] and $m_H \cong 125 \text{ GeV}/c^2$ [87].

We see that $\xi_w = \sqrt{\varphi^* \varphi} \leftarrow \xi_1$ is responsible for $m_W \leftarrow m_H$. Then, the $m_W \rightarrow m_{\ell, \bar{\ell}}$ is expected to reflect $\xi_w \rightarrow \xi_{\mp 1/2}$, which cooperates with the system transformation of $\| m \| = 1 \rightarrow m = \mp 1/2$, in which the confinement radius of Ψ_{\mp} is set to as $r = a \rightarrow a_{\mp 1/2}$. The base coupling $\sqrt{\varphi^* \varphi} = \xi_{\mp 1/2}$ is necessary for the regulated Ψ_{\mp} to properly couple with $U_{\mp}(\varphi^* \varphi)$. In the context, $\xi_1 \rightarrow \xi_{\mp 1/2}$ symbolically represents a process in which the rest mass $m_{\ell, \bar{\ell}}$ is

imprinted in our vacuum. When comparing $\xi = \xi_{-1/2} - \Delta\xi \rightarrow \xi_{-1/2}$ to mass renormalization of a charged lepton, $\xi \rightleftharpoons \xi_{-1/2}$ signifies self-complementation between the mass and charge renormalization.

We are tempted to relate the imprint of $m_{\ell, \bar{\ell}}$ to excitation of the φ -field in U_{\mp} . The excitation energies denoted as $\omega_{-1/2}$ and $\omega_{1/2}$ are given by

$$\omega_{-1/2} = U_{-}(\xi_{-1/2}) - U_{-}(\xi_w), \quad \omega_{1/2} = U_{+}(\xi_{1/2}) - U_{+}(\xi_w). \quad (65)$$

It is noted that if $\phi_1^2/\phi_{-1}^2 \sim \mathcal{O}(1)$, we have the relation of $\omega_{1/2} \ll \omega_{-1/2}$, because of $U_{+}(\xi_w) \approx U_{+}(\xi_{1/2})$ due to $\xi_w \sim \xi_{1/2}$. Equation (65) can be compared to the internal mass of Ψ_{\mp} analogous to meson mass. In this aspect, we invoke the Gell-Mann-Oakes-Renner relation indicating that m_{π}^2 is proportional to mass of the constituent quarks [55]. Combining these, we read ratio of $m_{\bar{\ell}}/m_{\ell}$ as reflection of $(\omega_{1/2}/\omega_{-1/2})^2 \cong 3.53 \times 10^{-6}(\phi_1^2/\phi_{-1}^2)^2$, and also, $a_{1/2}/a_{-1/2} = (\xi_{1/2}/\xi_{-1/2})(\omega_{-1/2}/\omega_{1/2})^2$. These values are estimated below.

6.3 The Electroweak Coupling

Reminding the form of the momentum operator that suffices for $SU(2) \times U(1)$ gauge invariance, we attempt at extending the indication of $\phi_{-1/2}^2 \rightarrow \alpha$ (Sect. 4.1): natural is to simply suppose $\phi_{-1}^2 \rightarrow g^2/q_P^2$ and $\phi_1^2 \rightarrow g'^2/q_P^2$, where g (g') is the coupling strength between the W (B^0) boson and the weak isospin (weak hypercharge) of left-handed (both-handed) particles. Therewith, the idea is that mode coupling among Φ_m , with ϕ_m being its strength, describes the electroweak coupling. At this juncture, we recall the orthogonal decomposition of $\kappa_{m(=m')}$ -spectrum: (ξ_m, k_m) . As we have seen that $m_H \rightarrow m_{\ell, \bar{\ell}}$ goes for ξ_m with $m = 1 \rightarrow \mp 1/2$, the $\tilde{\xi}$ -space is exhausted by coupling with matter fields. It is, therefore, reasonable to consider that the k -space left over is used for the concerned mode coupling, thereby yielding a representation of gauge field unification. Synchronizing with the mass pointer, $(g, g') \rightarrow e$ as charge pointer is to go for k_m with $m = \mp 1 \rightarrow -1/2$.

A vital clue to the relation between ϕ_m and k_m is found in the coupling of cylindrical functions of order $m = \pm 1$ (Sect. 3.1). An attention should be paid to the ratio of $c_{-1}^2/c_1^2 \sim \tilde{k}^4$, which plays a critical rôle in the quark confinement. Altogether, the confinement of Ψ_{-} inside the cylinder of $\Phi_{-1/2}$, which is compared to perfectly conducting wall, resembles the confinement of the color electric field as seen in the dual superconductor picture [88]. Hence, along the \tilde{k} -scaling form, we describe the multi-mode coupling among Φ_m . We here introduce the hyper coupling constant $\phi_p^2 [\sim (\xi_{-1/2}k_{-1/2})^{-4}]$, and hypothesize that the flows of Φ_m are self-adjusted in the way their intensities satisfy $\phi_m^2/\phi_p^2 = k_m^4$ each. Then, we have the chain rule for $m = -1/2, -1$, and 1, expressed as follows:

$$\phi_p^2 = \frac{\phi_{-1/2}^2}{k_{-1/2}^4} = \frac{\phi_{-1}^2}{k_{-1}^4} = \frac{\phi_1^2}{k_1^4}. \quad (66)$$

In particular, we obtain the ratio evaluated as

$$\phi_{-1/2}^2/\phi_{-1}^2 = (k_{-1/2}/k_{-1})^4 \cong 0.236. \quad (67)$$

This ratio is to be reflected in $e^2/g^2 = \sin^2 \theta_W$ in a low energy region, where θ_W is the weak mixing angle [44]. Indeed, the value of equation (67) agrees with the experimental data (marginally smaller than about 0.239 for the standard model) from atomic parity violation in sub- 10^{-2} GeV range (see figure 10.2 in [9], and references therein). Also, $\phi_1/\phi_{-1/2} = (k_1/k_{-1/2})^2 \cong 1.14$ is compared with g'/e , to be almost consistent with the corresponding ratio of m_Z/m_W , where m_Z the Z boson mass.

The numerical value of $m_{\bar{\ell}}/m_{\ell}$ works out, by letting $\phi_1^2/\phi_{-1}^2 = (k_1/k_{-1})^4$ in the foregoing expression of $(\omega_{1/2}/\omega_{-1/2})^2$, at 3.41×10^{-7} , and the one of $a_{1/2}/a_{-1/2}$, at 1.61×10^8 . Making the former ratio correspond to mass ratio of $\bar{\nu}_e$ to e^- , the $\bar{\nu}_e$ mass is estimated to be $m_{\bar{\nu}_e} \cong 174 \text{ meV}/c^2$, as consistent with the upper limit from direct neutrino mass experiment [89]. The experiment being in progress, or future planned ones [90, 91], could verify the proposed scenario.

7 Conclusions

In conclusion, I have proposed the internal geometric structure of point particles, which could capture the coupling with gauge fields and generate their intrinsic attributes. Infinitesimal realistic space with higher-dimensions has been supposed in a singular region of the point particles. I have suggested plasma dielectric (massive photon) picture of transformation between the internal space and our conventional space, as well as, magnetohydrodynamic (magnetic reconnection) picture of topological transformation of internal harmonic function. From the scalar-to-vector transformation, we have derived the rotational field capable of representing the Dirac's algebra. The vector field, which satisfies rotational eigenvalue equation, resides in the extra-dimensional space; it is updated recurrence of the Chandrasekhar-Kendall solution for Gromeka-Beltrami flow. The eigenflow that could be reflected in electromagnetic susceptibility has been investigated in details. A helical module representation of β^- -decay products has been provided in comparison with the Wigner's representation.

From the rotational eigenvalue equation, we have drawn a coordinate-rotor accommodated by the isotopic relation between complex orthogonal spaces. By turning the rotor, we have seen a mechanical sequence to maintain basis vectors in the spaces, as responsible for cyclotron motion of electron with its spin precession. It has been shown that the CSR (coordinate self-renormalization) process regulated by a specific rotational eigenvalue could be compared to charge renormalization. Within this framework, the CSR is found to, also, take on creating temporal degree of freedom, generating a numerical value

comparable to the electromagnetic coupling constant in low-energy limit. And, the new picture is obtained in which electrons embody reality of the geometric structure to ensure the scalar-intervening connection between our space and the infinitesimal space pertaining to another background.

Chiral asymmetry of the eigenflows has been connected with parity violation in weak interaction. A consequence is that the left-handed eigenflows $\Phi_{-1/2, -1}$ are involved in determining negative charge of lepton and quark, and multi-mode coupling of $\Phi_{-1/2, \mp 1}$ sustains the electroweak coupling, generating a numerical value comparable to the Weinberg angle measured at low energy. The theory suggests an internal landscape of $SU(3) \times SU(2) \times U(1)$ Yang-Mills fields plus Higgs vacuum, though it is speculative, and has only been compared with the partial structure of the quantum field theory at the moment. It is also notified that the following questions remain open: whether or not/how (1) this framework could respond to the higher energy including the so-called running and higher generation of leptons (related to higher order loop corrections of the anomalous magnetic moment), (2) the geometry could be connected with that of the other hypothetical theories, particularly, the string theory, (3) the CSR, with the general coordinate transformation, (4) the operational transformation, with the quantum measurements, and so forth.

In any case, the obtained results tentatively support the common picture of helical plasmas for the internal structure of point particles. Interestingly, the theoretical prototype seems to reveal some characteristics a parameter-free framework (if any, away from the anthropic principle [92, 93]) is likely to have. Regarding this, the extended scenario of determining the neutrino mass may be testable by laboratory experiments. I hope this work adds to particle physics in future, bringing a fresh perspective on structure of the Universe.

Acknowledgements This version of the article has been accepted for publication, after peer review (when applicable) but is not the Version of Record and does not reflect post-acceptance improvements, or any corrections. The Version of Record is available online at: <https://doi.org/10.1007/s10773-024-05717-5>. Use of this Accepted Version is subject to the publisher's Accepted Manuscript terms of use <https://www.springernature.com/gp/open-research/policies/accepted-manuscript-terms>

Author Contributions M.H. is the solo author of the manuscript.

Funding No funds, grants, or other support was received.

Data Availability All data generated or analysed during this study are included in this published article.

Declarations

Competing Interests The author declares no competing interests.

References

- [1] Halzen, F., Martin, A.D.: Quarks & Leptons: An Introductory Course in Modern Particle Physics. John Wiley & Sons, New York (1984)
- [2] Dehmelt, H.: A single atomic particle forever floating at rest in free space: new value for electron radius. *Physica Scripta T* **22**, 102–110 (1988). <https://doi.org/10.1088/0031-8949/1988/T22/016>
- [3] Gabrielse, G., Hanneke, D., Kinoshita, T., Nio, M., Odom, B.: New determination of the fine structure constant from the electron g value and QED. *Phys. Rev. Lett.* **97**, 030802 (2006). <https://doi.org/10.1103/PhysRevLett.97.030802>. (Erratum) **99**, 039902 (2007). <https://doi.org/10.1103/PhysRevLett.99.039902>
- [4] Gildener, E.: Gauge symmetry hierarchies. *Phys. Rev. D* **14**, 1667–1672 (1976). <https://doi.org/10.1103/PhysRevD.14.1667>
- [5] Nilles, H.P.: Supersymmetry, supergravity and particle physics. *Phys. Rep.* **110**, 1–162 (1984). [https://doi.org/10.1016/0370-1573\(84\)90008-5](https://doi.org/10.1016/0370-1573(84)90008-5)
- [6] Dimopoulos, S.: LHC, SSC and the universe. *Phys. Lett. B* **246**, 347–352 (1990). [https://doi.org/10.1016/0370-2693\(90\)90612-A](https://doi.org/10.1016/0370-2693(90)90612-A)
- [7] Canepa, A.: Searches for supersymmetry at the Large Hadron Collider. *Rev. Phys.* **4**, 100033 (2019). <https://doi.org/10.1016/j.revip.2019.100033>
- [8] The ATLAS Collaboration, Aad, G., et al.: Search for squarks and gluinos in final states with jets and missing transverse momentum using 139 fb⁻¹ of $\sqrt{s} = 13$ TeV pp collision data with the ATLAS detector. *J. High Energ. Phys.* **2021**, 143 (2021). [https://doi.org/10.1007/JHEP02\(2021\)143](https://doi.org/10.1007/JHEP02(2021)143) [arXiv:2010.14293 [hep-ex]]
- [9] Particle Data Group, Workman, R.L., et al.: Review of particle physics. *Prog. Theor. Exp. Phys.* **2022**, 083C01 (2022). <https://doi.org/10.1093/ptep/ptac097>
- [10] Letessier-Selvon, A., Stanev, T.: Ultrahigh energy cosmic rays. *Rev. Mod. Phys.* **83**, 907–942 (2011). <https://doi.org/10.1103/RevModPhys.83.907> [arXiv:1103.0031 [astro-ph.HE]]
- [11] Polchinski, J.: *String Theory*. Cambridge Univ. Press, Cambridge (1998)
- [12] Particle Data Group, Eidelman, S., et al.: Review of particle physics. *Phys. Lett. B* **592**, 1 (2004). <https://doi.org/10.1016/j.physletb.2004.06.001>
- [13] ATLAS Collaboration, Aad, G., et al.: Search for magnetic monopoles and stable high-electric-charge objects in 13 TeV proton-proton collisions

- with the ATLAS detector. *Phys. Rev. Lett.* **124**, 031802 (2020). <https://doi.org/10.1103/PhysRevLett.124.031802> [arXiv:1905.10130 [hep-ex]]
- [14] Gerlach, W., Stern, O.: Der experimentelle Nachweis der Richtungsquantelung im Magnetfeld. *Zeit. f. Phys.* **9**, 349–352 (1922). <https://doi.org/10.1007/BF01326983>
- [15] Planck, M.: Über das Gesetz der Energieverteilung im Normalspectrum. *Ann. d. Phys.* **4**, 553–563 (1901). <https://doi.org/10.1002/andp.19013090310>
- [16] Friedrich, J., Walcher, Th.: A coherent interpretation of the form factors of the nucleon in terms of a pion cloud and constituent quarks. *Euro. Phys. J. A* **17**, 607–623 (2003). <https://doi.org/10.1140/epja/i2003-10025-3> [arXiv:hep-ph/0303054]
- [17] Pauli, W. Jr.: Zur Quantenmechanik des Magnetischen Elektrons. *Zeit. f. Phys.* **43**, 601–623 (1927). <https://doi.org/10.1007/BF01397326>
- [18] Bohm, D.: *Quantum Theory*, Chap. 17. Prentice-Hall, Englewood Cliffs (1951)
- [19] Durrer, R., Neronov, A.: Cosmological magnetic fields: their generation, evolution and observation. *Astron. Astrophys. Rev.* **21**, 62 (2013). <https://doi.org/10.1007/s00159-013-0062-7>
- [20] Tajima, T., Shibata, K.: *Plasma Astrophysics*, Chap. 5. Addison-Wesley, Reading (1997)
- [21] Broderick, A.E., Loeb, A.: Signatures of relativistic helical motion in the rotation measures of active galactic nucleus jets. *Astrophys. J.* **703**, L104–L108 (2009). <https://doi.org/10.1088/0004-637X/703/2/L104> [arXiv:0908.2999 [astro-ph.HE]]
- [22] Woltjer, L.: A theorem on force-free magnetic fields. *Proc. Nat. Acad. Sci.* **44**, 489–491 (1958). <https://doi.org/10.1073/pnas.44.6.489>
- [23] Taylor, J.B.: Relaxation and magnetic reconnection in plasmas. *Rev. Mod. Phys.* **58**, 741–763 (1986). <https://doi.org/10.1103/RevModPhys.58.741>
- [24] Burlaga, L.F.: Magnetic clouds and force-free fields with constant alpha. *J. Geophys. Res.* **93**, 7217–7224 (1988). <https://doi.org/10.1029/JA093iA07p07217>
- [25] Plunkett, S.P., Vourlidas, A., Šimberová, S., Karlický, M., Kotrč, P., Heinzl, P., Kupryakov, Yu.A., Guo, W.P., Wu, S.T.: Simultaneous SOHO

- and ground-based observations of a large eruptive prominence and coronal mass ejection. *Solar Phys.* **194**, 371–391 (2000). <https://doi.org/10.1023/A:1005287524302>
- [26] Nambu, Y.: Quasi-particles and gauge invariance in the theory of superconductivity. *Phys. Rev.* **117**, 648–663 (1960). <https://doi.org/10.1103/PhysRev.117.648>
- [27] Goldstone, J.: Field theories with \ll superconductor \gg solutions. *Nuovo Cim.* **19**, 154–164 (1961). <https://doi.org/10.1007/BF02812722>
- [28] The Event Horizon Telescope Collaboration, Akiyama, K., et al.: First M87 event horizon telescope results. I. the shadow of the supermassive black hole. *Astrophys. J.* **875**, L1 (2019). <https://doi.org/10.3847/2041-8213/ab0ec7>
- [29] Ford, H.C., Harms, R.J., Tsvetanov, Z.I., Hartig, G.F., Dressel, L.L., Kriss, G.A., Bohlin, R.C., Davidsen, A.F., Margon, B., Kochhar, A.K.: Narrowband HST Images of M87: Evidence for a disk of ionized gas around a massive black hole. *Astrophys. J.* **435**, L27–L30 (1994). <https://doi.org/10.1086/187586>
- [30] Feynman, R.P.: *The Theory of Fundamental Processes*, Chap. 29. Addison-Wesley, Reading (1961)
- [31] Yang, C.N., Mills, R.L.: Conservation of isotopic spin and isotopic gauge invariance. *Phys. Rev.* **96**, 191–195 (1954). <https://doi.org/10.1103/PhysRev.96.191>
- [32] Anderson, P.W.: Plasmons, gauge invariance, and mass. *Phys. Rev.* **130**, 439–442 (1963). <https://doi.org/10.1103/PhysRev.130.439>
- [33] Wigner, E.: On unitary representation of the inhomogeneous Lorentz group. *Ann. Math.* **40**, 149–204 (1939)
- [34] Sommerfeld, A.: Zur Quantentheorie der Spektrallinien. *Ann. d. Phys.* **51**, 1–94 (1916). <https://doi.org/10.1002/andp.19163561802>
- [35] Beltrami, E.: Considerations on hydrodynamics. In: *Rendiconti del Reale Istituto Lombardo, Series II*, vol. 22 (1889). Filippini, G. (trans.) *Int. J. Fusion Energy* **3**(3), 53–57 (1985). <https://doi.org/10.1007/BF02719090>
- [36] Lee, T.D., Yang, C.N.: Question of parity conservation in weak interactions. *Phys. Rev.* **104**, 254–258 (1956). <https://doi.org/10.1103/PhysRev.104.254>

- [37] Wu, C.S., Ambler, E., Hayward, R.W., Hoppes, D.D., Hudson, R.P.: Experimental test of parity conservation in beta decay. *Phys. Rev. Lett.* **105**, 1413–1415 (1957). <https://doi.org/10.1103/PhysRev.105.1413>
- [38] Bostick, W.H.: Morphology of the electron. *Int. J. Fusion Energy* **3**(1), 9–52 (1985)
- [39] Eichten, E., Gottfried, K., Kinoshita, T., Lane, K.D., Yan, T.-M.: Charmonium: the model. *Phys. Rev. D* **17**, 3090–3117 (1978). <https://doi.org/10.1103/PhysRevD.17.3090>. (Erratum) **21**, 313 (1980). <https://doi.org/10.1103/PhysRevD.21.313.2>
- [40] Yukawa, H.: On the interaction of elementary particles. I. *Proc. Phys. Math. Soc. Japan* **17**, 48–57 (1935). <https://doi.org/10.1143/PTPS.1.1>
- [41] Gell-Mann, M.: A schematic model of baryons and mesons. *Phys. Lett.* **8**, 214–215 (1964). [https://doi.org/10.1016/S0031-9163\(64\)92001-3](https://doi.org/10.1016/S0031-9163(64)92001-3)
- [42] Higgs, P.W.: Broken symmetries and the masses of gauge bosons. *Phys. Rev. Lett.* **13**, 508–509 (1964). <https://doi.org/10.1103/PhysRevLett.13.508>
- [43] Glashow, S.L.: Partial-symmetries of weak interactions. *Nucl. Phys.* **22**, 579–588 (1961). [https://doi.org/10.1016/0029-5582\(61\)90469-2](https://doi.org/10.1016/0029-5582(61)90469-2)
- [44] Weinberg, S.: A model of leptons. *Phys. Rev. Lett.* **19**, 1264–1266 (1967). <https://doi.org/10.1103/PhysRevLett.19.1264>
- [45] Salam, A.: Weak and electromagnetic interactions. In: Svartholm, N. (ed.) *Elementary Particle Theory*, p. 367. Almqvist & Wiksell, Stockholm (1968)
- [46] Sakurai, J.J.: *Advanced Quantum Mechanics*. Addison-Wesley, Reading (1967)
- [47] Sir. Thomson, J.J.: The electrodeless discharge through gases. *Proc. Phys. Soc.* **40**, 79–89 (1927). <https://doi.org/10.1088/0959-5309/40/1/314>
- [48] Tonks, L., Langmuir, I.: Oscillations in ionized gases. *Phys. Rev.* **33**, 195–210 (1929). <https://doi.org/10.1103/PhysRev.33.195>
- [49] Einstein, A.: Zur Elektrodynamik bewegter Körper. *Ann. d. Phys.* **17**, 891–921 (1905). <https://doi.org/10.1002/andp.19053221004>
- [50] Einstein, A.: Die Grundlage der allgemeinen Relativitätstheorie. *Ann. d. Phys.* **49**, 769–822 (1916). <https://doi.org/10.1002/andp.19163540702>

- [51] Dirac, P.A.M.: General Theory of Relativity, Chap. 33. John Wiley & Sons, New York (1975)
- [52] Watson, G.N.: A Treatise on the Theory of Bessel Functions. Cambridge Univ. Press, London (1958)
- [53] Schwarzschild, K.: Über das Gravitationsfeld eines Massenpunktes nach der Einsteinschen Theorie. Sitzungsber. Preuss. Akad. Wiss. Berlin (Math. Phys.) **7**, 189–196 (1916)
- [54] Chew, G.F., Frautschi, S.C.: Regge trajectories and the principle of maximum strength for strong interactions. Phys. Rev. Lett. **8**, 41–44 (1962). <https://doi.org/10.1103/PhysRevLett.8.41>
- [55] Gell-Mann, M., Oakes, R.J., Renner, B.: Behavior of current divergences under $SU_3 \times SU_3$. Phys. Rev. **175**, 2195–2199 (1968). <https://doi.org/10.1103/PhysRev.175.2195>
- [56] Joukowski, N.E.: Über die Konturen der Tragflächen der Drachenflieger. Zeit. f. Flugtech. Motorluft. **1**, 281–284 (1910)
- [57] Bali, G.S.: QCD forces and heavy quark bound states. Phys. Rep. **343**, 1–136 (2001). [https://doi.org/10.1016/S0370-1573\(00\)00079-X](https://doi.org/10.1016/S0370-1573(00)00079-X)
- [58] Wilson, K.G.: Confinement of quarks. Phys. Rev. D **10**, 2445–2459 (1974). <https://doi.org/10.1103/PhysRevD.10.2445>
- [59] Hasegawa, A., Mima, K.: Stationary spectrum of strong turbulence in magnetized nonuniform plasma. Phys. Rev. Lett. **39**, 205–208 (1977). <https://doi.org/10.1103/PhysRevLett.39.205>
- [60] Honda, M., Meyer-ter-Vehn, J., Pukhov, A.: Collective stopping and ion heating in relativistic-electron-beam transport for fast ignition. Phys. Rev. Lett. **85**, 2128–2131 (2000). <https://doi.org/10.1103/PhysRevLett.85.2128>
- [61] Silva, L.O., Fonseca, R.A., Tonge, J.W., Dawson, J.M., Mori, W.B., Medvedev, M.V.: Interpenetrating plasma shells: near-equipartition magnetic field generation and nonthermal particle acceleration. Astrophys. J. **596**, L121–L124 (2003). <https://doi.org/10.1086/379156> [arXiv:astro-ph/0307500]
- [62] Honda, M.: Ultra-high energy cosmic-ray acceleration in the jet of Centaurus A. Astrophys. J. **706**, 1517–1526 (2009). <https://doi.org/10.1088/0004-637X/706/2/1517> [arXiv:0911.0921 [astro-ph.HE]]

- [63] Skyrme, T.H.R.: A non-linear field theory. Proc. Roy. Soc. Lond. A **260**, 127–138 (1961). <https://doi.org/10.1098/rspa.1961.0018>
- [64] Wess, J., Zumino, B.: Consequences of anomalous Ward identities. Phys. Lett. B **37**, 95–97 (1971). [https://doi.org/10.1016/0370-2693\(71\)90582-X](https://doi.org/10.1016/0370-2693(71)90582-X)
- [65] Witten, E.: Global aspects of current algebra. Nucl. Phys. B **223**, 422–432 (1983). [https://doi.org/10.1016/0550-3213\(83\)90063-9](https://doi.org/10.1016/0550-3213(83)90063-9)
- [66] Abrikosov, A.A.: The magnetic properties of superconducting alloys. J. Phys. Chem. Solids. **2**, 199–208 (1957). [https://doi.org/10.1016/0022-3697\(57\)90083-5](https://doi.org/10.1016/0022-3697(57)90083-5)
- [67] Parker, E.N.: Sweet’s mechanism for merging magnetic fields in conducting fluids. J. Geophys. Res. **62**, 509–520 (1957). <https://doi.org/10.1029/JZ062i004p00509>
- [68] Petschek, H.E.: Magnetic field annihilation. In: Hess, W.N. (ed.) The Physics of Solar Flares. Proceedings of the AAS-NASA Symposium held at the Goddard Space Flight Center, NASA SP-50, 425–439 (1964)
- [69] Horiuchi, R., Sato, T.: Self-organization process in three-dimensional compressible magnetohydrodynamics. Phys. Fluids **29**, 4174–4181 (1986). <https://doi.org/10.1063/1.865708>
- [70] Sato, T., the Complexity Simulation Group: Complexity in plasma: from self-organization to geodynamo. Phys. Plasmas **3**, 2135–2142 (1996). <https://doi.org/10.1063/1.871666>
- [71] Dirac, P.A.M.: The quantum theory of the electron. Proc. R. Soc. Lond. A **117**, 610–624 (1928). <https://doi.org/10.1098/rspa.1928.0023>
- [72] van der Waerden, B.L.: Group Theory and Quantum Mechanics, Chap. IV. Springer-Verlag, Berlin · Heidelberg (1974)
- [73] Chandrasekhar, S., Kendall, P.C.: On force-free magnetic fields. Astrophys. J. **126**, 457–460 (1957). <https://doi.org/10.1086/146413>
- [74] Moses, H.E.: Eigenfunctions of the curl operator, rotationally invariant Helmholtz theorem, and applications to electromagnetic theory and fluid Mechanics. SIAM J. Appl. Maths **21**, 114–144 (1971). <https://doi.org/10.1137/0121015>
- [75] Yoshida, Z., Giga, Y.: Remarks on spectra of operator rot. Math. Z. **204**, 235–245 (1990). <https://doi.org/10.1007/BF02570870>
- [76] Schumacher, B.: Quantum coding. Phys. Rev. A **51**, 2738–2747 (1995). <https://doi.org/10.1103/PhysRevA.51.2738>

- [77] Schrödinger, E.: Die gegenwärtige Situation in der Quantenmechanik. *Naturwissenschaften* **23**, 823–828 (1935). <https://doi.org/10.1007/BF01491914>
- [78] Aspect, A., Dalibard, J., Roger, G.: Experimental test of Bell's inequalities using time-varying analyzers. *Phys. Rev. Lett.* **49**, 1804–1807 (1982). <https://doi.org/10.1103/PhysRevLett.49.1804>
- [79] Hensen B., et al.: Experimental loophole-free violation of a Bell inequality using entangled electron spins separated by 1.3 km. *Nature* **526**, 682–686 (2015). <https://doi.org/10.1038/nature15759> [arXiv:1508.05949 [quant-ph]]
- [80] Schwinger, J.: On quantum-electrodynamics and the magnetic moment of the electron. *Phys. Rev.* **73**, 416–417 (1948). <https://doi.org/10.1103/PhysRev.73.416>
- [81] Witten, E.: String theory dynamics in various dimensions. *Nucl. Phys. B* **443**, 85–126 (1995). [https://doi.org/10.1016/0550-3213\(95\)00158-0](https://doi.org/10.1016/0550-3213(95)00158-0) [arXiv:hep-th/9503124]
- [82] Kaluza, Th.: Zum Unitätsproblem der Physik. *Sitzungsber. Preuss. Akad. Wiss. Berlin (Math. Phys.)*, 966–972 (1921). <https://doi.org/10.1142/S0218271818700017>
- [83] Klein, O.: Quantentheorie und fünfdimensionale Relativitätstheorie. *Zeit. f. Phys.* **37**, 895–906 (1926). <https://doi.org/10.1007/BF01397481>
- [84] Gross, D.J., Wilczek, F.: Ultraviolet behavior of non-abelian gauge theories. *Phys. Rev. Lett.* **30**, 1343–1346 (1973). <https://doi.org/10.1103/PhysRevLett.30.1343>
- [85] Politzer, H.D.: Reliable perturbative results for strong interactions? *Phys. Rev. Lett.* **30**, 1346–1349 (1973). <https://doi.org/10.1103/PhysRevLett.30.1346>
- [86] CDF Collaboration, Aaltonen, T., et al.: High-precision measurement of the W boson mass with the CDF II detector. *Science* **376**, 170–176 (2022). <https://doi.org/10.1126/science.abk1781>
- [87] ATLAS Collaboration, CMS Collaboration, Aad, G., et al.: Combined measurement of the Higgs boson mass in pp collisions at $\sqrt{s} = 7$ and 8 TeV with the ATLAS and CMS experiments. *Phys. Rev. Lett.* **114**, 191803 (2015). <https://doi.org/10.1103/PhysRevLett.114.191803> [arXiv:1503.07589 [hep-ex]]

- [88] Nambu, Y.: Strings, monopoles, and gauge fields. *Phys. Rev.* **10**, 4262–4268 (1974). <https://doi.org/10.1103/PhysRevD.10.4262>
- [89] The KATRIN Collaboration, Aker, M., et al.: Direct neutrino-mass measurement with sub-electronvolt sensitivity. *Nature Phys.* **18**, 160–166 (2022). <https://doi.org/10.1038/s41567-021-01463-1> [arXiv:2105.08533 [hep-ex]]
- [90] Esfahani, A.A., et al.: Determining the neutrino mass with cyclotron radiation emission spectroscopy–Project 8. *J. Phys. G* **44**, 054004 (2017). <https://doi.org/10.1088/1361-6471/aa5b4f> [arXiv:1703.02037 [physics.ins-det]]
- [91] Betti, M.G., et al.: Neutrino physics with the PTOLEMY project: active neutrino properties and the light sterile case. *J. Cosmol. Astropart. Phys.* **2019**, 047 (2019). <https://doi.org/10.1088/1475-7516/2019/07/047> [arXiv:1902.05508 [astro-ph.CO]]
- [92] Dicke, R.: Dirac’s cosmology and Mach’s principle. *Nature* **192**, 440–441 (1961). <https://doi.org/10.1038/192440a0>
- [93] Carter, B.: Large number coincidences and the anthropic principle in cosmology. In: Longair, M.S. (ed.) *Confrontation of Cosmological Theories with Observational Data*. International Astronomical Union / Union Astronomique Internationale **63**, Springer, Dordrecht (1974)